http://dx.doi.org/10.1097/mm9.0000000000000011

MedMat

Review

OPEN

Engineering programmable nanobiomaterials (PNBMs) for cancer nanotherapy

Jinghui Wang[a,b], Jiaxin Hou[a,b], Hangjie Lu[a,b], Sule Bai[a,b], Yu Chen[a,b], Wanting Yang[a,b], Shuo Wang[c], Guofeng Li[a,b], Yen Wei[d], Xing Wang[a,b], Wensheng Xie[a,b,*]

Abstract

With the rapid progress of nanotechnology, the development of multifunctional nanobiomaterials (NBMs) has brought about innovative strategies and improvements in tumor nanotherapy, particularly in achieving precise control over the therapeutic process for higher therapeutic efficacy while minimizing side effects. Considering the heterogeneous nature of the tumor microenvironment, NBMs need to be carefully regulated in terms of timing, location, and dosage. This gives rise to the concept of "programming nanobiomaterials (PNBMs)" to deliver the appropriate dose of drugs at the optimal time and site in response to endogenous or exogenous stimuli, thereby facilitating accurate tumor clearance. The objective of this article is to summarize current advances and applications of PNBMs in tumor nanotherapy. Additionally, it aims to discuss the utilization of PNBMs in tumor precision therapy in terms of component programming, size programming, hydrophilicity programming, cascade response programming, logic gate control programming, and multifactor response programming. Furthermore, we prospect the PNBMs fusion design, matching complicated microenvironments, degradability and safety, and clinical application potential, all of which will serve as a reference for the design and development of novel and efficient PNBMs in cancer nanotherapy.

Keywords: PNBMs, cancer nanotherapy, spatiotemporal control, engineering design

1. NBMs and programmable design

Nanomaterials hold enormous promise for biomedical applications due to their unique nanoscale effects and surface characteristics, such as high specific surface area, multifunctionality, and biocompatibility.[1,2] These features render nanomaterials intriguing for a wide range of applications, including drug delivery, gene therapy, and tissue engineering.[3–8] Since the beginning of the 21st century, research on nanobiomaterials (NBMs) has become more in-depth and extensive, especially considering the rapid growth of precision medicine, which has increased the demand for medicinal materials.[9,10] Precision medicine and personalized medicine focus on patient-centeredness, formulating treatment strategies based on individual distinctions and the peculiarities of patients' diseases. This treatment model necessitates medical materials that can accurately recognize and respond to the patient's biological signals to achieve precise diagnosis and treatment.[11–13] Driven by this demand, the concept of programmable nanobiomaterials (PNBMs) has emerged. PNBMs aim to achieve precise control over the behavior of materials within organisms through precise programming of components, structures, and functions, thereby better meeting the needs of precision medicine and personalized medicine.

The definition of PNBMs is not confined to NBMs that can be precisely controlled and regulated by external signals such as optical, electrical, magnetic ultrasonic, mechanical, or chemical signals. They represent a new class of smart materials with the capability to be precisely programmed in terms of components, structure, and function.[14–17] This programming ability enables PNBMs to respond to external stimuli at precise doses under specific spatial and temporal conditions to perform specific biological functions. (1) Component programmability: the chemical composition of PNBMs can be precisely designed and adjusted as required. This involves the selection of appropriate biocompatible materials, the addition of specific bioactive molecules (eg, drugs, antibodies, and enzymes), and the optimization of the material's composition ratio. Through component programmability, precise control of the bioactivity of PNBMs can be achieved to meet different therapeutic or diagnostic requirements.[18–21] (2) Structural programmability: the morphology, size, and surface properties of PNBMs can be precisely designed and adjusted as needed. This encompasses controlling the shape (eg, spherical, rod-shaped, and star-shaped), size (from a few nanometers to hundreds of nanometers), and surface modifications (eg, hydrophilicity, hydrophobicity, and targeting) of the nanoparticles (NPs). Structural programmability enables PNBMs to interact more effectively with organisms and enhances their stability and bioavailability in vivo. By precisely controlling the structure of PNBMs, precise regulation of

Jinghui Wang, Jiaxin Hou, Hangjie Lu, Sule Bai, and Yu Chen have contributed equally to this work.

[a]State Key Laboratory of Organic-Inorganic Composites, College of Life Science and Technology, Beijing University of Chemical Technology, Beijing, China, [b]Beijing Laboratory of Biomedical Materials, Beijing University of Chemical Technology, Beijing, China, [c]China-Japan Friendship Hospital, Beijing, China, [d]The Key Laboratory of Bioorganic Phosphorus Chemistry & Chemical Biology (Ministry of Education), Department of Chemistry, Tsinghua University, Beijing, China.

**Corresponding author: Address: State Key Laboratory of Organic-Inorganic Composites, College of Life Science and Technology, Beijing University of Chemical Technology, Beijing 100029, China. E-mail address: xws@mail.buct.edu.cn (W. Xie).*

MedMat (2025) 2:1

Received: 16 December 2024; Accepted 12 January 2025

Published online 20 January 2025

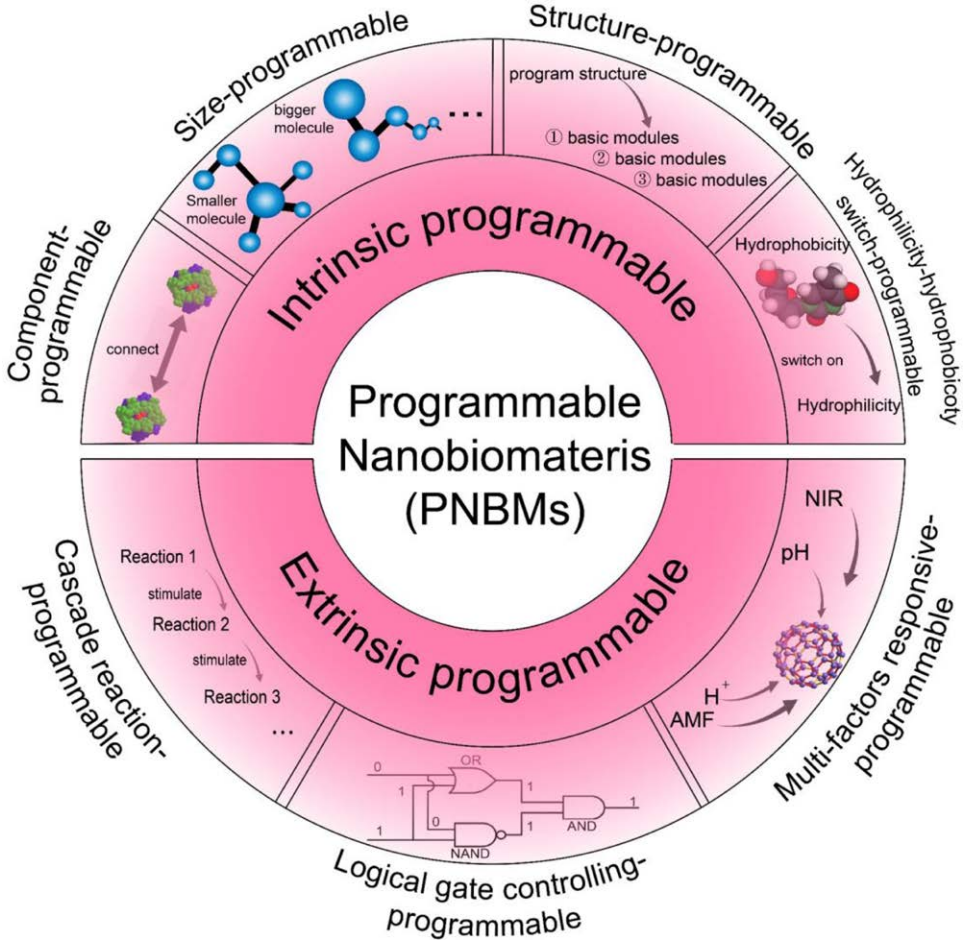

Figure 1. The design of programmable nanobiomaterials (PNBMs) for cancer nanotherapy via intrinsic programmable and extrinsic programmable strategies.

their distribution and behavior in the organism can be accomplished.[22–25] (3) Functionally programmable: this entails the realization of specific functions such as biorecognition, targeting, release, and response. Through functional programmability, precise control of the behavior of PNBMs within organisms can be achieved, leading to precise diagnosis and treatment of diseases. In terms of precise spatiotemporal, and dosage control, functionally PNBMs are capable of responding to specific biological signals or stimuli to release drugs or perform other biological functions at precise dosages and time points.[22,26–28]

PNBMs possess the following advantages. (1) Targeting: programmable switches can accurately identify cancer cells and selectively trigger the therapeutic response, reducing the damage to healthy cells and effectively decreasing the toxic side effects of the treatment.[29] (2) Adjustability: the intensity and timing of the treatment can be adjusted according to the patient's specific situation, enabling personalized treatment, improving the therapeutic effect, and reducing the risk simultaneously.[30,31] (3) Effectiveness: programmable switches can enhance the treatment's effectiveness, reduce tumor resistance, and improve the survival rate and quality of life of patients.[32,33] (4) Sustainability: programmable switch technology can control the treatment in a long-term and stable manner, prevent tumor regeneration and recurrence, and prolong the survival time of the patients.[34–36] (5) Technological frontier: programmable switches are among the frontier technologies in the field of medical science currently, which have a high research and development potential, and are expected to become an important means of cancer treatment in the future.[37,38] In this review, we have collected and reviewed a large number of studies on PNBMs and related programmable switches to provide a detailed description of the programmability of programmable switches, including intrinsic programmable design and extrinsic programmability (Figure 1). Intrinsic programmable design involves component, size, structure, and hydrophilic and hydrophobic programmability, while extrinsic programmability includes cascade reaction, logic gate control, and multifactor-responsive programmability. We explain the principles of these programmability aspects and discuss their potential applications in cancer therapy. The purpose of this article is to serve as a reference for the design and development of novel and efficient PNBMs in cancer nanotherapy.

2. Intrinsic programmable design of PNBMs

2.1 Component programmable

Component programmability represents a technique for attaining programmability through the modification of materials composition or the implementation of modularization.[39–41] By adding or subtracting specific components, the properties of the material can be artificially regulated, which is usually influenced by factors such as hydrophilicity and steric hindrance.[42–44] Peptide-based supramolecular self-assembly has been shown to be a flexible approach to fabricate programmable nanodrugs by employing synergistic or reciprocal intermolecular noncovalent interactions.[43,45–47]

For example, Zhang et al.[48] succeeded in changing the self-assembly and a variety of properties of materials by varying the amount of unsaturated linoleic acid (LA) at the N-terminal end of lipopeptides. They used NH_2-D(KLAKKLAK)-$CONH_2$ (P1) as the original material and generated LA-D(KLAKKLAK)-$CONH_2$ (P2) and $(LA)_2$-D(KLAKKLAK)-$CONH_2$ (P3) by introducing LA to couple with the peptide within the resin. These modified materials are capable of self-assembling into spherical structures and exhibit better aggregation effects and cationic properties than P1, resulting in more effective contact with anionic membranes and stronger antitumor effects. In addition, these materials are less susceptible to degradation outside the tumor environment (TME) and have good tumor-targeting properties (Figure 2A). Similarly, Mout et al.[52] tuned the properties of the materials by varying the amount of proteins in the hydrogels. They designed hydrogel precursors containing different protein units (a designed homodimer denoted as C2, a designed homopentamer denoted as C5, a 24-chain tetrahedral nanocage denoted as T33, and a 120-chain icosahedral nanocage denoted as I53) and connected them by variable length flexible linkers (Gly-Gly-Ser). It was found that the stiffness of the hydrogels increased as the length of the flexible linker (GGS)n joints increased. In terms of the rigidity arm, the storage modulus increased dramatically as the length increased from 1.0 nm to 7.5 nm. Besides, the C2 × I53 combination was able to form gels rapidly in a short time in terms of the chemotaxis, whereas the C2 × T33 combination formed gels on a longer time scale. For both the C2 × T33 and C2 × I53 combinations, the energy storage modulus decreases with increasing (GGS)n joint length, which is in contrast to the results for the smaller C5 cores, whose stiffness increases with increasing joint length. These findings suggest that precise control of material properties can be achieved by fine-tuning of the material's components.

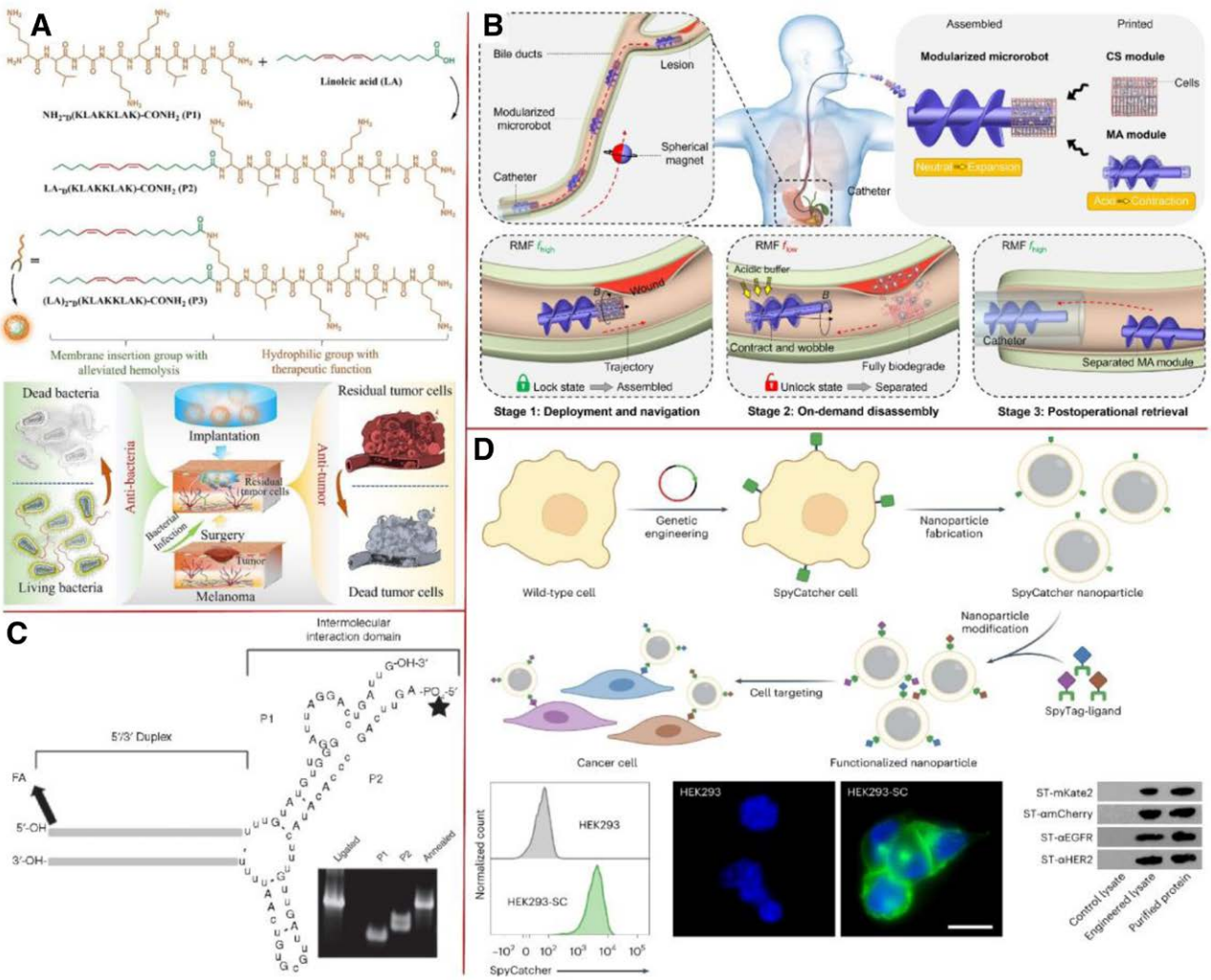

Figure 2. Component programmable PNBMs. (A) A schematic representation for the application of lipopeptide nanotherapy achieved through the programmed synthesis of lipopeptides in the tandem treatment of postoperative infections and recurrence in melanoma patients. Adapted with permission from Zhang et al.,[48] © 2023 Elsevier B.V. (B) A schematic depiction of programmable nanorobots utilized in tumor therapy, achieved through the incorporation of diverse functional modules. Adapted with permission from Su et al.,[49] © 2023 Springer Nature Limited. (C) Control cellular pRNA nanoparticles comprising P1 and P2 RNA sequences, with folic acid selectively conjugated to the 5'-ends of both P1 and P2. Adapted with permission from Abdelmawla et al.,[50] © 2011 Elsevier B.V. (D) The results of flow cytometry evaluation of wild-type HEK293 cells and HEK293 cells expressing SpyCatcher are presented. A fluorescence-based method was utilized to observe SpyCatcher expression in wild-type HEK293 cells and HEK293-SC cells. Cell nuclei were stained with DAPI and showed blue fluorescence, while SpyCatcher fused with sfGFP showed green fluorescence. Detection of SpyTag-labeled ligands by Western blotting. Adapted with permission from Krishnan et al.,[51] © 2024 Springer Nature Limited.

Component programmability is not limited to changing a single component but also involves giving a material a new function by introducing different modules. This modular approach allows one to replace functional modules and thus artificially control the functionality of the material.[53,54] For example, Su et al.[49] developed a microrobotic system for multifunctional targeted cell delivery. These microrobots consist of a magnetic actuation (MA) module with active mobility and a cell scaffold (CS) module with biocompatibility and biodegradability. Their programmability is reflected in the relative sizes of the CS and MA modules as well as the selective carrying of CS-like modules with different functions. The motion patterns of the microrobot, such as forward, backward, turn, and roll, change its assembly state depending on the difference between the CS aperture and MA size. There exists a critical size of 160 μm. When the difference is higher than this critical value, the locking between the MA and CS modules can be maintained firmly regardless of the motion patterns, while when the difference is lower than 160 μm, the MA module may be easily detached from the CS module, especially during turning and rolling motions, which may lead to the failure of the assembled microrobot (Figure 2B). Krishnan et al.[51] developed cell membrane-coated nanoparticles (CNPs), which enable the programmability of CNPs by attaching different modules to the cell membrane for modification. They experimented with 4 modules: the fluorescent protein mKate2, designed ankyrin repeat protein (DARPin) targeting mCherry (denoted as αmCherry), DARPin targeting epidermal growth factor receptor (EGFR) (denoted as αEGFR), and DARPin targeting growth factor receptor (HER2) (denoted as αHER2). These modules were further modified with SptTag to form ST-mKate2, ST-αmCherry, ST-αEGFR, and ST-αHER2. The results showed that αmCherry-NPs (αmCherry-coupled nanoparticles) had no significant cellular interactions. Whereas both αEGFR-NPs and αHER2-NPs could effectively target cells, SC-NPs had limited cellular interactions. In terms of tumor therapy, docetaxel (DTX) is encapsulated into a self-assembled poly(lactic-co-glycolic acid) (PLGA) core via hydrophobic interactions to form αmCherry-[DTX] NPs. The corresponding targeted nanoformulations showed high inhibition rates for tumor growth. Similarly, αEGFR-[DTX] NPs and αHER2-[DTX] NPs were effective for tumor growth inhibition, whereas SC-[DTX] NPs had a much smaller effect (Figure 2D). In addition, Abdelmawla et al.[50] constructed an RNA NP based on the packaging RNA (pRNA) of the phage phi29 DNA packaging motor, which can be folded into a dense structure and self-assembled by a dichotomous approach to form a nanodelivery system. Such pRNA NPs can be modularized without altering the folding properties, with the modular sites located at the 5' ends of P1 and P2 (the entire pRNA molecule was split into 2 segments, designated as P1 and P2, at a cleavage site situated at the 3′ end of nucleotide number 55). For example, Cy5-pRNA-folic acid monomer NPs formed by introducing folic acid into the 5' end of P2 or P1 and self-assembling can be used to target cancer cells carrying the folate receptor. This study demonstrates that 2'-F-modified pRNA NPs with multiple functional modularities can be easily fabricated by this scalable dichotomous strategy (Figure 2C).

In the context of tumor photothermal therapy (PTT), Chang et al.[55] found that programming the amino acid sequence of self-assembled peptides could efficiently achieve tumor ablation and thus improve the therapeutic efficacy of PTT. To this end, 3 typical dipeptides, diphenylalanine (FF), dityrosine (YY), and diaspartic acid (DD) were employed to illustrate the effect and also included aspartic acid (D) and tetraaspartic acid (DDDD) to assess the effect of changing the number of amino acids. Pheophorbide a (PheoA), a hydrophobic chlorophyll derivative was selected as the model photosensitizer. Finally, they synthesized 5 conjugates, PheoA-D (PD), PheoA-DD (PDD), PheoA-DDDD (PDDDD), PheoA-FF (PFF), and PheoA-YY (PYY). Nanostructures showed that PFF formed spherical NPs with an average size of 70 nm, whereas all other conjugates formed nanofibers (NFs) with a persistent length of up to 15 μm and a diameter of 25 nm. It was shown that the structural stability of PD-NFs was superior to that of PDD-NFs and PDDDD-NFs and that this increased stability could be attributed to enhanced hydrophobic effects, whereas the difference between PYY-NFs and PFF-NPs could be attributed to enhanced intermolecular hydrogen bonding. The increased structural stability of PD-NFs and PYY-NFs ensures their tumor selectivity in the biological environment, accumulation, efficient cellular internalization, and high photothermal conversion rates in the biological environment. The treatment results showed effective tumor ablation without tumor recurrence or detectable side effects. Meanwhile, the differences in phototherapeutic activity depend on their different cellular internalization and catabolic behaviors in the physiological environment. This study reveals that noncovalent interactions can be thought to be designed by programming the amino acid sequence to artificially design superior PTT drugs.

2.2 Size programmable

Size regulation of nanomedicines is a crucial area of research in cancer therapy. Variation in size not only affects the delivery efficiency of the drug but also its biodistribution in the body. In drug delivery systems, the size of a drug molecule has a significant impact on its behavior in the body. Smaller molecules of drugs can pass through obstacles in the bloodstream more easily and reach cancer cells faster, while larger molecular drugs may move slower through the body. Previous studies suggested that larger molecular drugs are more likely to accumulate in tumor tissue, which may make them more efficient in treating cancer.[56–58] In addition, the size of the drug molecule may modulate the rate and duration of drug release in the body. Larger molecules of a drug may release the drug slowly, but their effects are sustained for a longer period of time. This property means that by precisely controlling the size of a drug molecule, the biodistribution and efficacy of the drug can be optimized, thereby improving the effectiveness of cancer treatment. However, refining this size-modulation technique presents several challenges, including accurately controlling the size of the drug molecule and ensuring its stability within the body.

The size programmability of PNBMs can directly affect the drug delivery efficiency. A mixture of positively and negatively charged mixed-charge NPs can selectively target lysosomes in cancer cells while exhibiting only minimal cytotoxicity to normal cells. This selectivity is driven by pH-dependent aggregation events, beginning with the formation of small, easily endocytosed clusters on the cell surface and culminating in the assembly of large, ordered NP polymers and crystals within the cancer lysosome.[59] These assemblies cannot be cleared by the cytosolic process, leading to lysosomal swelling, gradual disruption of lysosomal membrane integrity, impairment of lysosomal function, and eventual induction of cell death. As mentioned in the referenced study, in contrast to pure cationic/pure *N*,*N*,*N*-trimethyl(11-mercaptoundecyl) ammonium chloride nanodrug carriers, [+/–] drug carriers gradually accumulate in vivo, and

eventually accumulate in acidic environments at sites that have a destructive and functionally impairing effect on cancer lysosomes. The size of the [+/–] drug carriers is controlled to manipulate their aggregation process in the approximate pH 5.5 to 7.0 range. This allows the drug to exist as a larger number of intermediate-sized (~50–100 nm) carriers. It is this aggregation behavior that allows [+/–] drug carriers to form clusters on the surface of cancer cells. Upon undergoing increasingly acidic intracellular lysosomal pathways, the small aggregates of [+/–] drug carriers initially produced on the cell surface fuse into larger aggregates and eventually form crystals within the lysosome.[60] In another study, thioketals modified DOX (TDOX), triphenylphosphine (TPP), and indocyanine green (ICG) were conjugated to poly (amidoamine) (PAMAM), a highly branched molecule, by electrostatic attraction, and then synthesized DIT (DOX-ICG-TPP)-PAMAM was conjugated to polyethylene glycol grafted poly lactic acid (PEG-g-PLA) to form the nanocarrier PEG-PLA@DIT-PAMAM by electrostatic repulsion effect. This nanocarrier has low cytotoxicity, high biocompatibility, and tumor targeting. The following text discusses the change in size of the nanocarriers after incubation with glutathione (GSH).[61] By measuring the particle size distribution of the NPs, it was found to be divided into 2 main fractions: small-sized particles (about 30 nm, close to the diameter of DIT-PAMAM of 25.8 nm) and large-sized particles (particle sizes from 800 to 10,000 nm). When centrifugation was performed, the ζ-potential of the solution increased from 6.9 mV to 16.2 mV, indicating that the nanocarriers had been disintegrated, releasing positively charged NPs of various sizes. Transmission electron micrographs observed that the morphology of the nanocarriers changed and the size of the NPs varied from 23.9 nm to ~190 nm, demonstrating that the DIT-PAMAM NPs could react with the PEG-PLA copolymer chains with opposite charges. After incubation with GSH, transmission electron microscope (TEM) images showed almost complete dissociation of the composite micelles, which was consistent with the dynamic light scattering (DLS) results.[62–64] These results suggest that in the tumor microenvironment, the size variation of the nanocarriers has a significant effect on their drug delivery efficiency.

Size-modulated changes in carriers are also an approach to treating cancer, but it is a challenge to ensure that drug molecules remain stable in vivo. Lee et al. created programmable prodrug carriers for chemotherapy/photodynamic therapy (PDT)/PTT against nasopharyngeal carcinoma to enhance photostability and bypass biochemical barriers (Figure 3B).[64,66] These nanocarriers have size-shrinkable and charge-reversal properties that enhance tumor penetration and produce highly regulated local drug release. In their study, the size change of the molecule Cy7-tricyanofuran (TCF)-tk-indomethacin (IMC) was explored.[67,68] It was demonstrated that Cy7-TCF-tk-IMC could

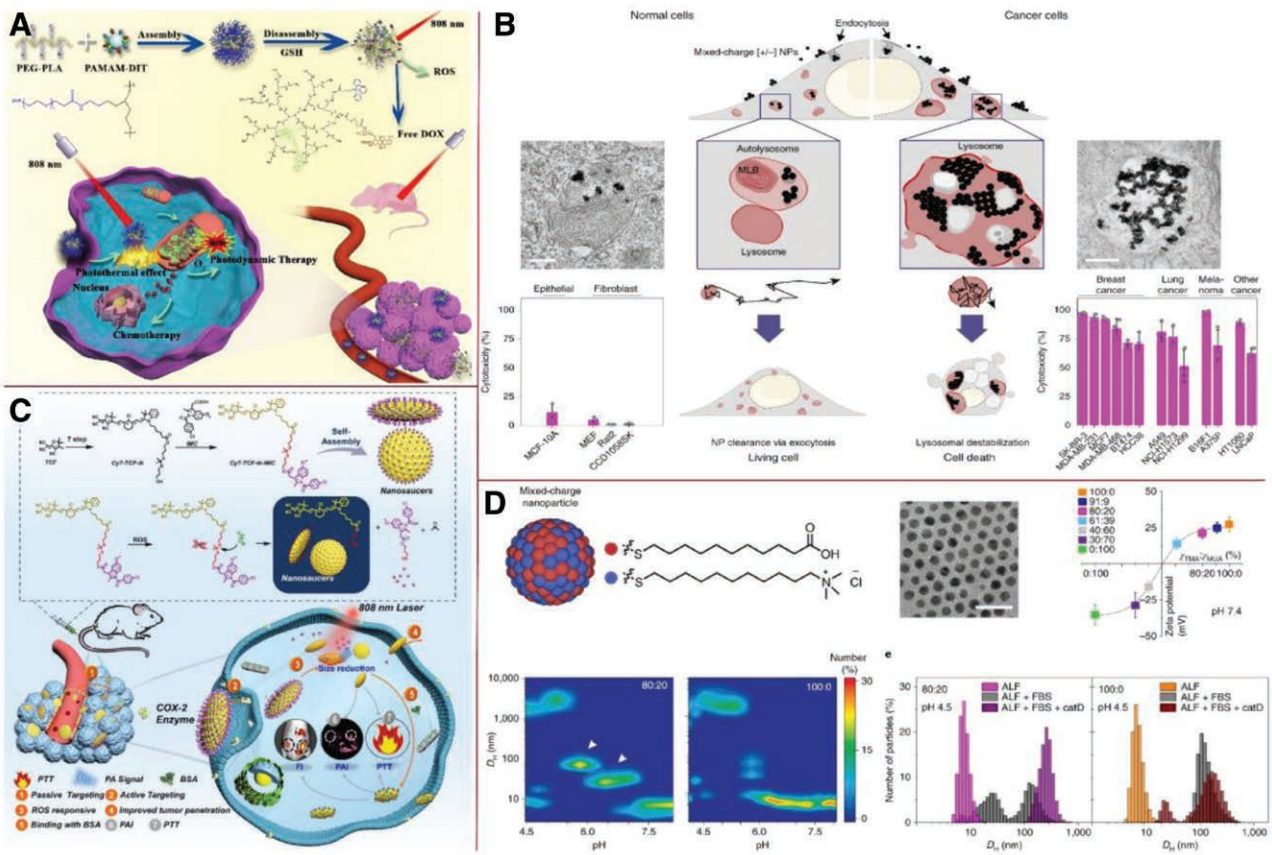

Figure 3. Size programmable PNBMs. (A) The fabrication process involves the integration of PEG-g-PLA copolymers with DIT-PAMAM nanoparticles, followed by the controlled release of DIT-PAMAM from the resultant PEG-PLA@DIT-PAMAM nanocomposite within a tumor microenvironment abundant in GSH. Adapted with permission from Cheng et al.,[61] © 2023 Elsevier B.V. (B) The synthesis of Cy7-TCF-tk-IMC was successfully achieved, accompanied by a schematic diagram that illustrates the structural configuration of Cy7-TCF-tk-IMC. Adapted with permission from Cheng et al.,[61] © 2023Elsevier B.V. (C) The crystallization process of mixed-charge nanoparticles within cancer cell lysosomes, ultimately resulting in the selective elimination of cancer cells. Adapted with permission from Borkowska et al.,[65] © 2020 Springer Nature Limited. (D) The investigation focuses on the structural characteristics of the surface charge mixing in nanoparticles, along with their aggregation behaviors as a function of pH levels. Adapted with permission from Borkowska et al.,[65]© 2020 Springer Nature Limited.

form stable NPs at very low concentrations. DLS was used to monitor the particle size of Cy7-TCF-tk-IMC NPs in deionized water. No significant size change was observed after 24 hours of incubation, demonstrating that the Cy7-TCF-tk-IMC NPs were extremely stable. After H_2O_2 (10 mM) treatment, the average size of the NPs decreased from ~125 to ~75 nm, which could be attributed to the cracking of the IMC and stronger intermolecular π–π stacking interactions between Cy7-TCF-SH (sulfhydryl group) after the removal of IMC. TEM images showed that the morphology of Cy7-TCF-tk-IMC NPs was a well-defined spherical shape both before and after treatment. Atomic force microscopy analysis revealed that the thickness of these spherical particles was consistently smaller than the diameter, suggesting a disc-shaped nanostructure. These results suggest that changes in size and morphology may have an impact on the efficacy of Cy7-TCF-tk-IMC in cancer diagnosis and treatment.[69–71]

The size of PNBMs can be influenced by programming to affect the efficiency of drug delivery. Mixing charged NPs with both positive and negative charges can selectively target lysosomes in cancer cells while showing only marginal effects on the toxicity of normal cells (Figure 3A). This selective targeting is driven by pH-dependent aggregation events, starting with the formation of small, easily internalized clusters on the cell surface, followed by the assembly of larger and more ordered NP polymers and crystals within the lysosomes of cancer cells. These larger assembled bodies cannot be cleared through exocytosis, leading to swelling of the lysosomes and progressive damage to the integrity of the lysosomal membrane, impairing its function and ultimately inducing cell death. Literature has reported that compared to pure cationic or TMA nanodrug carriers (which produce toxicity without selectivity to cells), the aggregation behavior of [+/–] drug carriers in vivo is more complex.[72–74] In acidic environments, they eventually accumulate in the lysosomes of cancer cells, thereby causing damage and functional impairment to the lysosomes. The size of the drug carrier is tightly controlled and manipulated within the pH range of 5.5 to 7.0.[60] This regulation enables the drug to exist in intermediate sizes of aggregated clusters (approximately 50–100 nanometers) in large numbers, effectively enhancing its drug delivery capacity. It is this aggregation behavior that enables [+/–] drug carriers to form clustered structures on the surface of cancer cells. As the intracellular environment gradually becomes acidic, these initial small aggregates formed on the cell surface will fuse into larger aggregates and eventually form crystals within the lysosomes (Figure 3D). Initially, the aggregation process of the drug carrier is assisted by slightly negative charges on blood serum proteins. As the pH decreases, the negative charges on the drug carrier promote the formation of these aggregates through hydrogen bonds or van der Waals forces.[65]

2.3 Structure programmable

Structural programmable is a design that focuses on module functionality and processing.[40,75] This approach follows a top-down strategy of gradual refinement, dividing the program structure functionally into a number of basic modules that are functionally relatively independent and have simple relationships. Each module consists of 3 fundamental structures: sequential, selective, and cyclic. The implementation of modularization typically depends on the use of subroutines. Structured program design effectively reduces the design difficulty by decomposing the complex program system design task into several easy-to-manage and handle submodules through module decomposition and functional abstraction. Structured programmable design for PNBMs has prominent application scenarios in both tumor imaging and therapy. In the field of tumor imaging, Zhao et al.[76] prepared DNA-Mn hybrid nanoflowers (DMNFs) via a manganese ion-mediated enzymatic biomineralization method. During the self-assembly of these DMNFs, the nucleation and growth of Mn^{2+} can be artificially controlled in a "top-down" manner, which in turn affects the structure and function of the products. By adjusting the concentration of Mn^{2+} and the reaction time, the morphology and structure of DMNF can be changed. For example, after 24 hours of reaction at different Mn^{2+} concentrations, the morphology of the biomineralization products evolved from a multiplate structure at 0.5 mM Mn^{2+} concentration to a flower-like structure at 6 mM Mn^{2+}, and ultimately to irregular aggregates at 10 mM Mn^{2+}. As the concentration of Mn^{2+} increases, the size of the product gradually decreases. In contrast, extending the reaction time results in an increase in DNA content, which can serve as a template for biomineralization and promote the growth of PPi_4 paraproducts within the flower-like framework (Figure 4A, B). In tumor therapy, Li et al.[79] adjusted the self-assembly ability by changing the length of the branched fatty alcohol of the prodrug, reflecting the idea of "top-down, step-by-step" structural programmability. They linked 7-ethyl-10-hydroxycamptothecin (SN38) with branched aliphatic alcohol (BAA) of different chain lengths via disulfide bonds to form SN28-BAA precursors of different lengths, which could self-assemble into spherical NPs. It was found that SN38-C21 NPs (SN38-11-heneicosanol nanoparticles) with the longest BAA chain exhibited the best antitumor effect and the least toxicity. In terms of cellular uptake, SN38-C15 NPs were rapidly taken up due to their fast release rate, while SN38-C21 NPs were more frequently captured by cells due to their hydrolysis resistance and stability.

In addition to achieving structural programmability by modifying the prodrug or process, a multilevel structure was designed, which is a composite system composed of several structural units at different levels. In this system, the main structure is divided into several basic modules, and simple relationships are established between these modules.[80,81] For example, by loading drugs with different properties (eg, hydrophilicity and hydrophobicity) into material sites with corresponding properties, a drug delivery system carrying drugs with multiple properties can be realized.[82–84] This approach helps to reduce the amount of drug used and is programmable by adjusting the molar ratio of the drugs carried.[85–88] Typically such materials have properties such as pH responsiveness.[89–91] Chen et al.[78] designed a water-soluble amphiphilic oleic acid-NaYF4:Yb,Er/polydopamine gold nanoflower Janus nanoparticles (OA-UCNPs/PDA-AuF JNPs) with discrete multicompartmental nanostructures as dual-drug delivery systems. This fulfills the requirement of containing hydrophobic hydroxycamptothecin (HCTP)/hydrophilic doxorubicin (DOX) in the partitioned space and releasing each drug from the noninterfering channel under dual pH/near-infrared (NIR) stimulation. HCPT was loaded into hydrophobic UCNPs, while DOX was loaded into the PDA fraction. The materials were pH-responsive as well as programmable in terms of molar ratio: the synergistic effect was optimal when the fixed molar ratio of HCPT/DOX-loaded OA-UCNPs/PDA-AuF JNPs was HCPT: DOX = 1:1. At pH 7.4, only 24% of HCPT and 26.5% of DOX were released from the loaded OA-UCNPs/PDA-AuF JNPs within 104 hours. In contrast, at pH 5.3, ~87.1% of DOX and 60.5% of HCPT were released. The main reason for this phenomenon is the protonation

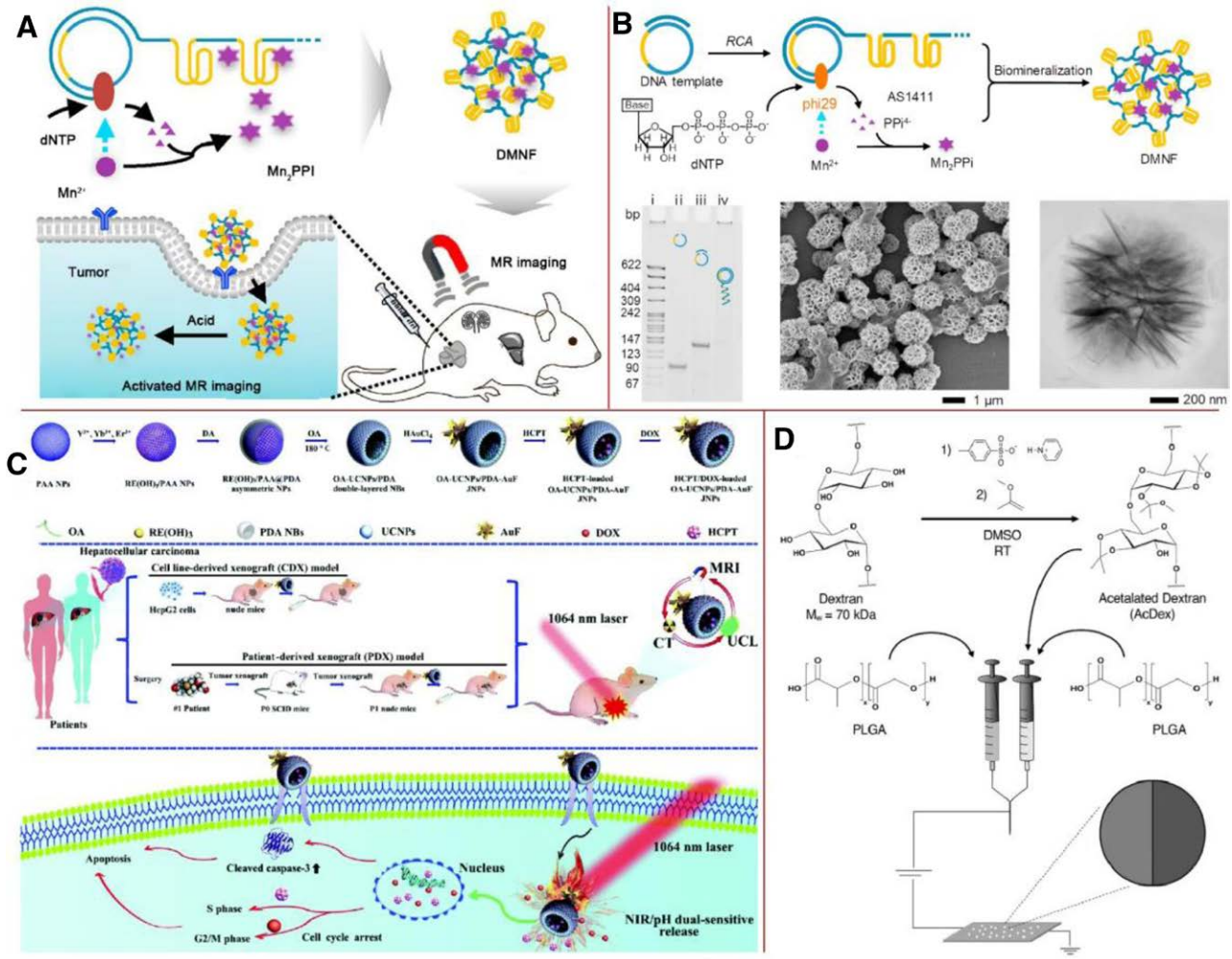

Figure 4. Structure programmable PNBMs. (A) Schematic diagram of the role of DMNFs. Adapted with permission from Zhao et al.,[76] © 2024 Elsevier B.V. (B) A schematic illustration depicting the formation of DMNF (discontinuous minifilament) facilitated by the phi29 DNA polymerase enzyme. Adapted with permission from Zhao et al.,[76] © 2021 Elsevier B.V. (C) The reaction scheme outlines the chemical synthesis pathway for the preparation of pH-responsive acetal dextran. Adapted with permission from Gregory et al.,[77] © 2020 Wiley Online Library. (D) Schematic diagram of OA-UCNPs/PDA-AuF JNPs loaded into HCPT/DOX with CDX and PDX modeling. Adapted with permission from Chen et al.,[78] © 2021 Elsevier B.V.

of the NH2 group in DOX, which accelerates the release of the drug from the PDA fraction at pH 5.3. For HCPT, it may be because it becomes more hydrophilic and water soluble at low pH, resulting in more release of HCPT from the OA-UCNPs fraction into an aqueous solution (Figure 4C). Similarly, Gregory et al.[77] created a dual-compartment JNP that achieves drug release for 2 different therapies on the same pH-responsive release NP platform. By varying the molar ratio of lapatinib (LAP) to paclitaxel (PTX), the release capacity could be adjusted. When the PTX dose was low, the molar ratio of LAP:PTX was synergistic at a molar ratio greater than 1 (combinatorial index <1). However, the synergistic effect decreases with a significant increase in PTX dose (Figure 4D).

2.4 Hydrophilicity–hydrophobicity switch programmable

Controlling the hydrophilicity of drugs is key to improving drug efficacy and selectivity. Many drug molecules are inherently hydrophobic, which makes them difficult to disperse in the hydrophilic environment of the body. Therefore, the development of drug carriers with hydrophilic properties is essential to improve drug delivery efficiency. These carriers can effectively encapsulate hydrophobic drug molecules and help them reach the tumor site through the bloodstream. First, to enhance drug selectivity, hydrophobic molecules typically exhibit selective distribution within the body, preferentially accumulating in specific tissues or cells. By utilizing this property, hydrophobic drug molecules or carriers can be designed to accumulate mainly in cancer cells, improving drug selectivity and reducing damage to normal cells.[62] Second, to control drug release, the rate of drug release in vivo can be influenced by regulating the hydrophobicity of drug molecules or carriers. Hydrophobic drug molecules are usually released at a slower rate in vivo, and sustained drug release can be achieved by regulating hydrophobicity. Although the control of hydrophobicity offers the potential for effective therapy, maintaining the stability of drug molecules or carriers in different in vivo environments remains a challenge.

Vallejo-Sánchez et al.[92] explored the preparation of metal-organic frameworks (MOFs) via a phase-transfer strategy and described in detail how the structure and properties of these MOFs can be influenced by modulating the hydrophilic nature (Figure 5A). Scanning electron microscopy images showed that the structure of the MOFs was transformed from the granular structure of the MONPs to the fiber-type structure after

incubation in water for 15 min, which showed a significant effect of the change of hydrophilic and hydrophobic properties on the structure of the MOFs. In contrast, when Zn^{2+} and dithiooxamidato (DTA) were mixed directly in water without a phase-transfer process, MOFs could not be formed at room temperature, but a large amount of precipitate was formed at the bottom of the reaction test tube.[93,94] Self-supported MOFs are formed when the reaction temperature is increased to 80 °C, which highlights the important role of environmental transfer in the preparation of MOFs. The study also examined in detail the relationship between the surface hydrophilicity of the NPs and their pharmacokinetics, exploring how an increase in surface hydrophilicity enhanced their blood circulation time.[95] The distribution of the NPs in the bloodstream was observed by in vivo microscopy time series imaging. For NPs labeled with 1,1'-dioctadecyl-3,3,3',3'-tetramethylindodicarbocyanine (DiD), it was found that as the hydrophilicity of the NP surface increased, its circulation time in the bloodstream gradually increased. This suggests that the highly hydrophilic PMOEEP (poly(2-methoxyethy-2-oxo-1,3,2-dioxaphospholane)) polymer shell layer delays the clearance of NPs by immune cells. The fluorescence of NPs mixed with different ratios of polycaprolactone (PCL)-b-PMOEEP in plasma was further examined by an in vivo microimaging system, and the results showed that NPs containing more PCL-b-PMOEEP exhibited a longer blood circulation time (Figure 5B). In addition, the effect of surface hydrophilicity on the accumulation of NPs in tumors was also investigated. The experimental results demonstrated that, due to its enhanced surface hydrophilicity, the accumulation of n-PMOEEP@DiR NPs in tumors following intravenous injection was significantly increased, with fluorescence still detectable even 72 hours postinjection. And in n-PMEP@DiR (poly(2-methy-2-oxo-1,3,2-dioxaphospholane) [PMEP]) and n-PEEP@DiR (poly(2-ethoxy-2-oxo-1,3,2-dioxaphospholane) [PEEP]) NPs, the tumor accumulation tended to increase as the proportion of PCL-b-PMOEEP polymer increased. In conclusion, the high hydrophilicity of the NP surface prolonged the blood circulation time and increased the accumulation of tumors, which may further improve drug delivery and therapeutic efficacy.[96–99]

3. Extrinsic programmable design of PNBMs

3.1 Cascade reaction programmable

A cascade reaction is a chemical reaction in a series of consecutive events in which the former event can stimulate the latter. Cascade reaction in the study of PNBMs is mainly concerned with how to release different drugs step by step under different environments or stimuli.[27] Currently, common solutions include both multiresponsive and logic-gated approaches, which exhibit great potential for precise tumor therapy. These applications include the design of responsive nanocarriers for specific release of drugs at the tumor site, PTT/PDT using light-activated cascade reactions, and immunotherapy that triggers the activation and immune response of immune cells.[100] The significance of these approaches is to improve therapeutic efficacy, enhance drug targeting to tumor cells, reduce damage to normal tissues, improve efficacy through synergistic strategies, and personalize therapy to tailor treatment.

The principle of multiresponse reaction allows different drug factors to be output by modulating different input instructions. The advantage of this approach is that different PNBMs can be designed for more accurate drug delivery while protecting healthy cells by premeasuring the environment in the vicinity of the target. In recent years, several research teams have invented a variety of novel multiresponsive PNBMs for cancer therapy. For example, ultra-small platinum nanoparticles (USPtNs) can kill cancer cells by leaching Pt ions into acidic organelles. However, due to the short half-life in vivo and toxicity to other normal tissues of such Pt nanomedicines smaller than 5 nm, it is difficult to achieve mass-targeted delivery.[101,102] Gemcitabine (GEM) and cisplatin are common drug combinations to inhibit cancer cell growth. Shi et al.[103] prepared a pH/redox dual stimulation-responsive clustered NP for simultaneous delivery of USPtNs and GEM for the treatment of nonsmall cell lung cancer (Figure 6A). This clustered NP (GP-NA) consists of a disulfide bond-containing GEM graft copolymer, a pH-sensitive peptide, and USPtNs. This hybrid nanosystem performs multiple functions within cancer cells, including the production of cytotoxic Pt ions in response to the acidic environment of lysosomes and the release of GEM in the reducing environment of the cytoplasm. This mechanism minimizes GEM damage to normal cells while ensuring more precise drug delivery in TMEs, thereby protecting healthy cells and effectively targeting cancer cells. Cancer-associated fibroblasts (CAFs) produce a significant amount of extracellular matrix (ECM), which leads to poor permeability of therapeutic drugs and creates an immunosuppressive tumor microenvironment. As a result, therapeutic agents struggle to effectively penetrate the area surrounding cancer cells for treatment. Li et al.[104] developed a green nanomodulator oleanolic acid (OA)-rose bengal (RB)-methylene blue (MB) (ORM) based on OA nanogel combined with the supersensitizer RB and the photothermal agent MB, which enabled more accurate access of therapeutic factors to the target sites through a 3-pronged deep intratumoral penetration and TME modulation. OA itself inactivates CAFs, while light irradiation promotes the disassembly and degradation of matrix-bound collagen, remodeling the ECM. This process increases osmotic pressure and triggers the release of RB. Following the release of RB, acoustic kinetic therapy is enhanced by ultrasound, resulting in a cascading response from the 3 therapies that inhibit the growth of cancer cells.

The logic gate response principle allows 2 or more logic gates to be independently designed on a single PNBM system and edited to realize different commands to output different contents. For instance, Tang et al.[105] edited 2 different logic gates in a single nanovesicle for on-demand chemotherapy (Figure 6B). One logic gate paralleled mild thermotherapy and acidic pH to perform NIR laser-triggered prodrug-to-drug conversion via Edman degradation. A second logic gate enables programmable drug release via a single stimulus input to the NIR laser. The biodistribution of nanovesicles was monitored by positron emission tomography, photoacoustic, and fluorescence imaging to precisely regulate drug release while scanning the lesion. Zhou et al.[106] developed a cryptobiotic-inspired pH/adenosine triphosphate (ATP) "AND" enzyme logic gate platform for tumor-specific drug delivery (Figure 6C). By preventing contact between the DOX-conjugated gelatin (DG) NP and enzymes with durable tannic acid-Fe (TA-Fe), the obtained DG@TA-Fe is expected to exhibit cryptogenic behavior in healthy tissues with negligible premature drug leakage. Once reaching the tumor region, the mildly acidic pH and/or upregulated ATP in the tumor microenvironment would first release TA-Fe, followed by hydrolysis of the exposed internal DG core by matrix metalloproteinase 2/9overexpressed in the solid tumor region to release cytotoxic DOX.

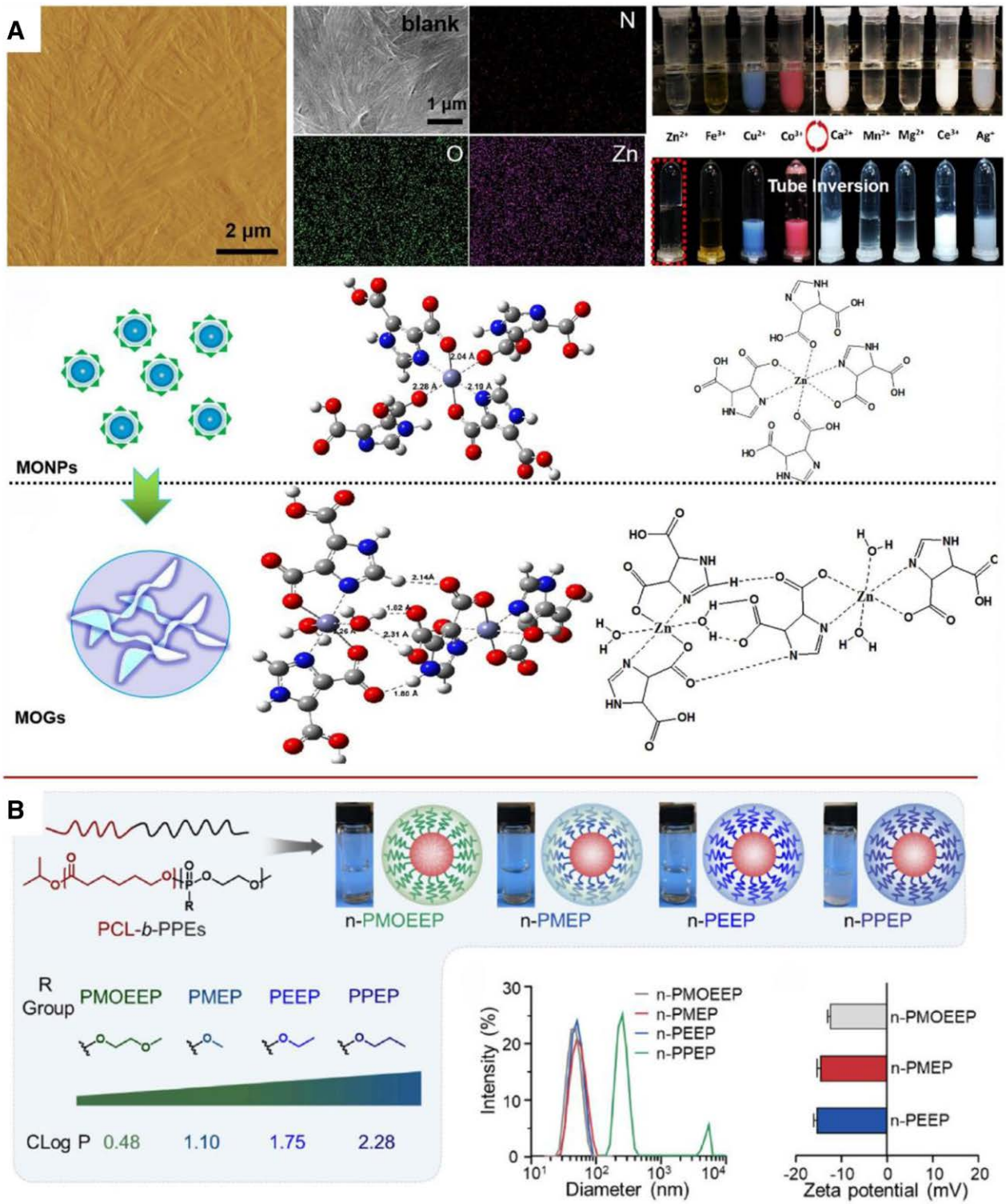

Figure 5. Hydrophilicity–hydrophobicity switch programmable PNBMs. (A) Elemental mapping of brine-induced metal-organogels (MOGs) and optimized structures and possible coordination mechanisms of DTA and Zn^{2+} in methanol and water. Adapted with permission from Vallejo-Sánchez et al.,[92] Copyright © 2017 Wiley Online Library. (B) Schematic of the chemical structure and synthesis of PPE ethylated nanoparticles highlighting the oil–water partition coefficient of the PPE pendant moiety. Particle size distributions and zeta potentials of the nanoparticles were characterized using DLS analysis and cryogenic transmission electron microscopy images were acquired for n-PMOEEP, n-PMEP, and n-PEEP. Images were collected and their particle size profiles were then quantitatively analyzed. Adapted with permission from Lu et al.,[57] © 2020 American Chemical Society.

3.2 Logic gate controlling programmable

The combination of logic gates and PNBMs applied in the field of cancer therapy is an emerging research direction with the goal of solving the problem of precision in drug delivery. By predesigning logic gate circuits, it is possible to achieve targeted drug release outcomes based on specific input parameters. The successful development of this method addresses the previous challenges of achieving precise drug delivery and drug combination. It enhances the efficacy of drug delivery and action during

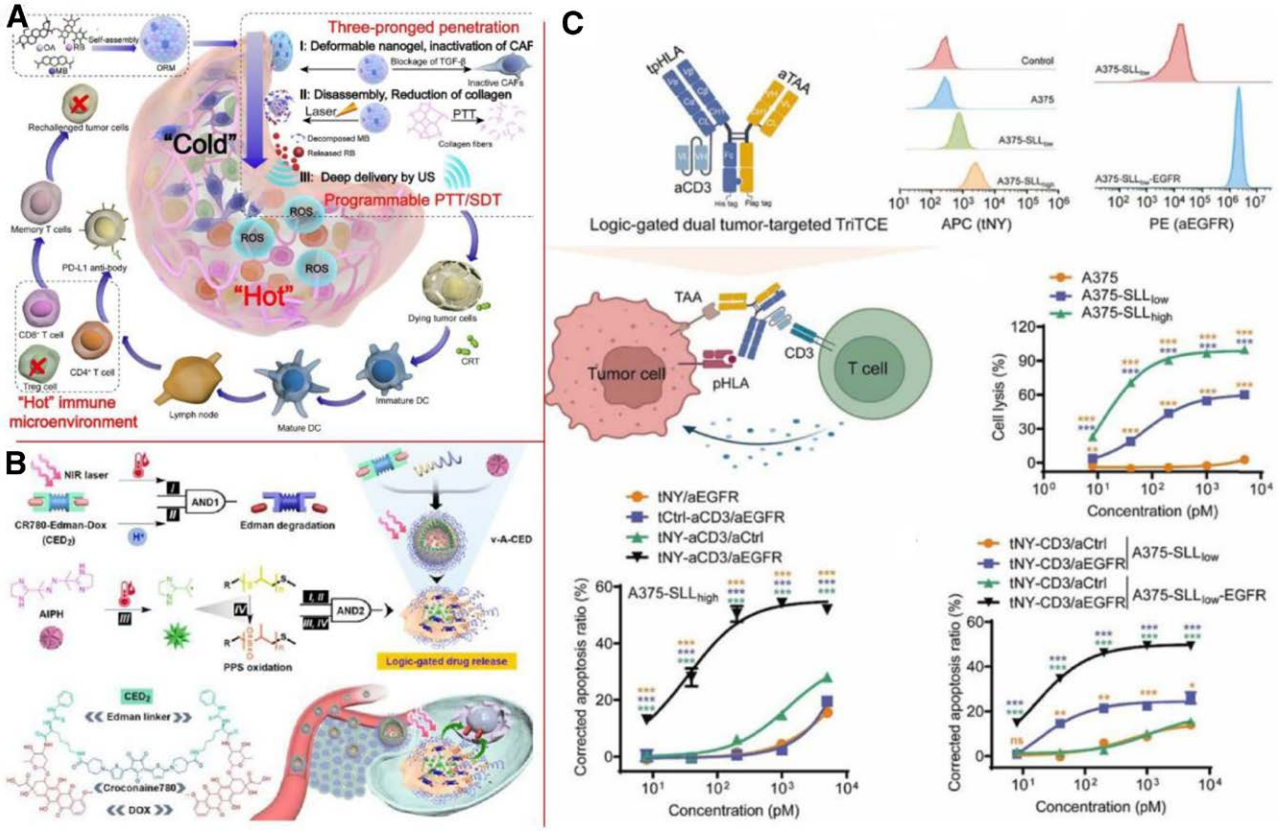

Figure 6. Cascade reaction programmable PNBMs. (A) Schematic representation of a 3-pronged strategy for ORM-enhanced tumor penetration in programmable PTT/sonodynamic therapy (SDT)-assisted anti-PD-L1 (programmed cell death ligand 1) immunotherapy. Adapted with permission from Li et al.,[104] © 2022 Elsevier B.V. (B) Schematic diagram of logic-gated drug release from modular nanoparticles (v-A-CED2) for on-demand chemotherapy. Adapted with permission from Tang et al.,[105] © 2019 Ivyspring International Publisher. (C) Design and in vitro antitumor activity of logically gated dual tumor-targeting TriTCEs and schematic representation of the conformation of logically gated dual tumor-targeting TriTCEs. Adapted with permission from Zhou et al.,[106] © 2023 Elsevier B.V.

the treatment process while minimizing the risk of significant accidental damage to healthy cells, which is often associated with traditional therapeutic modalities in cancer treatment. A safer and healthier tumor treatment is achieved through procedures set in advance.

In the traditional concept of logic gates, there are several types of logic gates. However, the main logic gates used for drug delivery in oncology are "or" and "and" gates. Researchers have utilized both parallel and serial logic gates to integrate these 2 types of logic gates for drug delivery, aiming to achieve more accurate and safer drug administration. Parallel logic gates facilitate the combination of drugs in tumor therapy, enhancing both functionality and efficacy. In contrast, tandem logic gates enable precise target delivery, minimize drug loss, improve drug utilization, and reduce the side effects of medications on the human body. Li et al.[107] developed an artificial light-controlled logic-gated transmembrane K-selective channel based on single-chain random heteropolymers that incorporate molecular motors (Figure 7). They constructed an artificial logic-gated transmembrane K-selective channel containing "NOT" gate components. At the core of these gates are photosensitive molecular motors capable of undergoing reversible E-Z conformational transitions or photo-oxidative dissociation into indanone derivatives (Figure 7A). The modulation of the different operational modes of the 3 logic gates was achieved by employing light sources with varying wavelengths from 310 to 365 nm, as well as artificially created aerobic and anaerobic environments to control the variables. This approach enabled the state switching of the K-translocating capacity. Furthermore, stepwise-controlled K transport and apoptosis-inducing activities were conducted using the logic gate circuits. The results demonstrated that a series of responses induced by K-cell exocytosis could lead to the apoptosis of cancer cells. In this study, the logic gate operates normally when it is in the "ON" state, and when a specific condition is input to put the logic gate in the "Partially OFF" and "Totally OFF" states, the logic gate will operate in the "Partially OFF" and "Totally OFF" states (Figure 7B, C). The rapid exocytosis of K leads to cellular vacuolization, loss of mitochondrial membrane potential, and release of cytochrome c from mitochondria into cytoplasmic lysate, which ultimately induces apoptosis in cancer cells (Figure 7D).

Understanding how the 2 types of logic gates work and their effects is essential for achieving design objectives. This approach enhances the circuit's fault tolerance and speed while providing the flexibility to meet various logic requirements. Although fewer teams have conducted related research, some significant results have been achieved. For instance, Bai et al. developed a molecular logic gate (MLG)-modulated core crosslinked predrug system with combined dual-stimulus response properties. In the absence of a reducing agent, the AND logic gate closes under neutral pH conditions, inhibiting the release of DOX. Upon internalization of the NPs into cancer cells, the cellular environment causes the logic gates to open and release DOX. PEG-SS-DOX conjugates were synthesized and confirmed through a 2-step reaction, with Cu^{2+} selected as the dynamic crosslinking agent. The pH and reduction

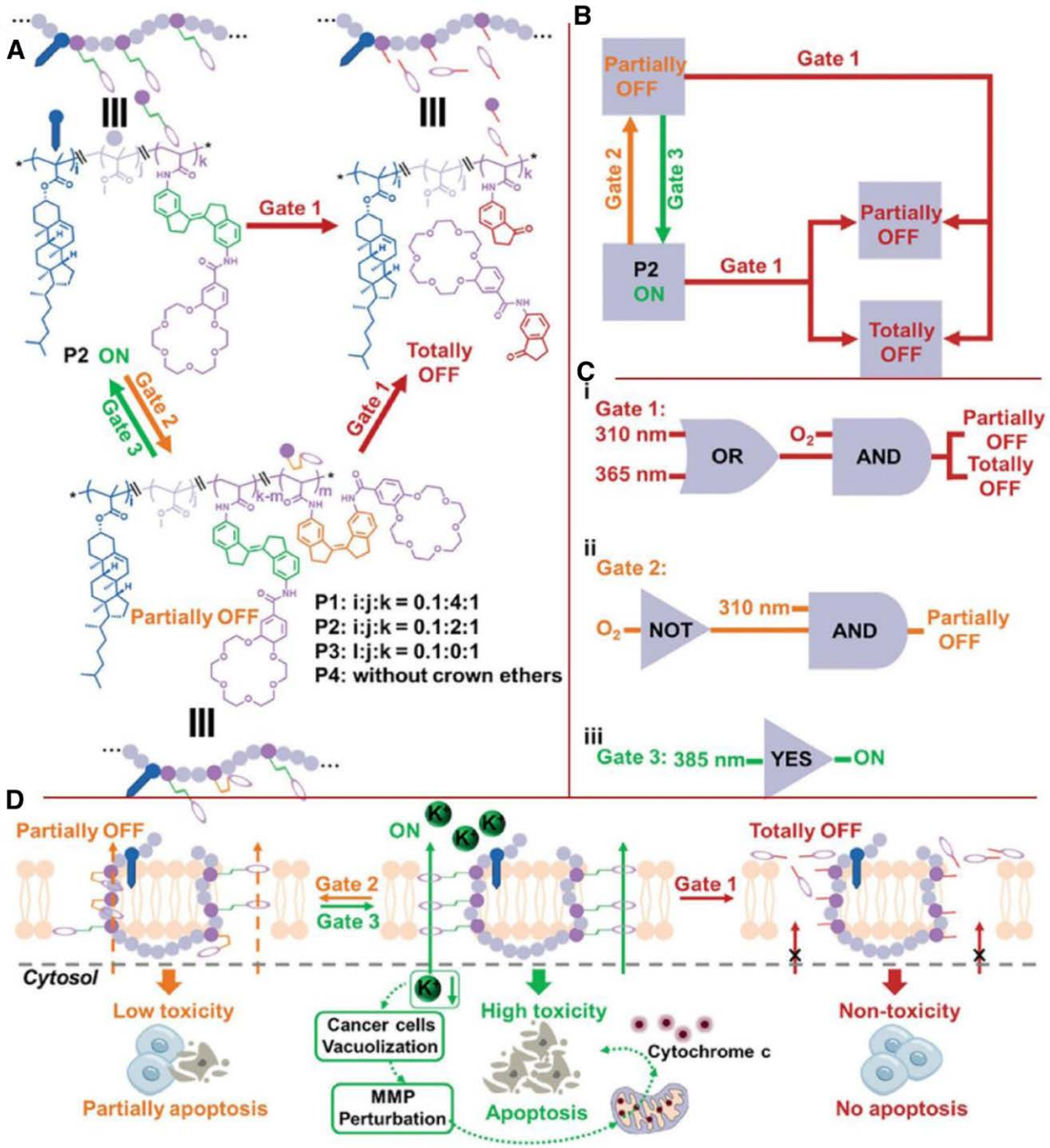

Figure 7. Combined schematic diagram of a novel light-controlled logic-gated artificial transmembrane ion channel system for stepwise control of K^+ transporter and cancer cell apoptosis. (A) Chemical modifications and schematic representations of P2 subsequent to the implementation of "Gate 1," "Gate 2," and "Gate 3" instructions are presented. The variables i, j, and k denote the proportions of the 3 monomers, namely (E)-M1, M2, and M3, in the polymerization process. (B) Schematic diagram of P2 to illustrate the change in K^+ transmission capability after performing a logic gate operation. A "partial shutdown" in yellow font indicates a reversible state and a "partial shutdown" in red font indicates an irreversible state. (C) The construction of "YES," "OR," "WITH," and "NO" gates involves the utilization of oxygen and various wavelengths of light as input signals. The output signal is represented by the capability of P2 to transport K^+. (D) A schematic depiction of a P2 system that utilizes molecular motors, exhibiting tunable transport activity. This system is designed to deliver anticancer therapeutics, with its operational modality being governed by logic gate manipulation. Adapted with permission from Li et al.,[107] © 2024 Elsevier B.V.

dual-reaction drug release behavior of the precursor system were investigated. There was no significant difference in the cumulative release of noncrosslinked precursors under varying pH conditions. The premature release of the drug was inhibited by Cu^{2+} crosslinking. Although the release rate increased under acidic conditions, the cumulative release remained below 40%. The release rate was enhanced by Cu^{2+} crosslinking, but the cumulative release still did not exceed 40%. Strengthening the reduction signal could activate the AND logic gate to trigger the release. The findings of this research can facilitate more accurate and rapid targeted drug delivery, prevent premature responses, and improve the efficiency of anticancer prodrug

utilization.[108] The initial introduction of the MLG ("AND") concept has garnered significant attention. The primary research and development focus of these 2 teams is to integrate the MLG with PNBMs for the targeted delivery of cancer therapeutic drugs. The research done by Li et al.[107] aims to regulate the release of K^+ ions to induce apoptosis in cancer cells, thereby enhancing the efficacy of cancer therapies while minimizing the adverse effects of these drugs on the human body. Meanwhile, Bai's team is working to improve the selectivity of cancer drug targeting, thereby achieving more precise drug delivery.[108]

3.3 Multifactor response programmable

Multifactor-responsive programming is a method for inducing predictable changes in drug carriers or the drug itself by manipulating various external factors to achieve efficient drug delivery and targeted therapy. Recent research advancements have demonstrated that exogenous factors such as light, magnetism, and specific ion concentrations can be utilized to modulate drug release. The management of these external factors can be classified into single-factor control and multifactor control, enabling more precise treatment of tumors.

Among them, the use of exogenous light and magnetic field to manipulate PNBMs has achieved more mature research results.[109–111] For example, Qiao et al.[112] prepared a family of multiresponsive nanogels by the miniemulsion copolymerization of monomethyl oligo(ethylene glycol) acrylate and an ortho ester-containing acrylic monomer in the presence of a disulfide-containing crosslinker (Figure 8A). These nanogels could be programed by thermo/pH/redox factors. The acid-triggered swelling performance and thermo-programmable properties were contributed by the composition and crosslinking degree, and the reductive degradability was brought by the disulfide linkage. These nanogels may find applications as carriers for the site-specific delivery of hydrophobic antitumor drugs. Gheata et al.[116] proposed a system based on lithium niobate harmonic nanoparticles (LNO HNPs) that modulates the morphology of the system to achieve on-demand drug release by laser excitation at different wavelengths as an exogenous stimulus. The resulting nanocouplings (LNO-CM-ELA NPs) were successfully imaged in EGFR overexpressing human prostate cancer cells DU145 by detecting the second harmonic emission at 625 nm in a tissue transparent window. Tuning the laser to 790 nm resulted in the uncaging of the ELA cargo, facilitating the on-demand release of the drug. Fuller et al.[113] described magnetically controlled nanocarriers (MCNCs) that release heat and drug cargo under an applied alternating magnetic field (AMF) (Figure 8B). The release is programmable and modulated by the AMF field strength and can be spatially controlled using a selective magnetic field gradient. The MCNC platform facilitates the combination of superparamagnetic iron oxide nanoparticles (SPION) and engineered polymers with thermally unstable drug couplings, creating stable carriers with controlled size, drug-carrying efficiency, drug-carrying capacity, and both passive and triggered release rates. Experiments confirmed the temperature-dependent modulation of MCNC release; specifically, the release varied with external heating at 37 °C in a 25/75 v/v methanol/PBS release medium or after 1 hour in AMF at temperatures of 45 °C, 52.5 °C, and 60 °C.

In addition to the unifactorial control of light and magnetism, specific ion concentrations can be used as external factors for multifactorial control. Li et al.[114] implemented a programmable nanoreactor FeS_2@PcD based on specific Fe^{3+} responsive phthalocyanine PcD and FeS_2 NPs for fluorescence and magnetic resonance dual-modal imaging-guided acoustic/chemical kinetic therapy (Figure 8C). The FeS_2@PcD in the TME programmed by pH and H_2O_2 showed highly specific activation. A "bivariate factor" of H^+ and H_2O_2 resulted in a 7.76-fold or 0.39-fold increase in fluorescence intensity, exceeding the previously reported bivariate factor-enhanced fluorescence intensity. Huang et al.[115] engineered an engineered programmable spiking by the coordination-driven coassembly of Evans blue, copper ions, and 5-hydroxy-*p*-naphthoquinone (HND) shaped nanogenerator (Figure 8D). This nanogenerator for oxidative stress-based antitumor therapy is capable of rapidly decomposing and releasing drugs in response to the dual stimulation of acidic lysosomes and endogenous GSH after effective enrichment and internalization into tumor cells in the tumor region. In addition, the released HND not only effectively amplifies endogenous H_2O_2 via intracellular oxidoreductase but also downregulates Pin 1 activity, providing excellent antitumor effects.

4. Conclusion and outlooks

In summary, this article delves into the engineering of PNBMs, which aims to achieve meticulous control over the timing, spatial distribution, and dosage in cancer nanotherapy through the programmable design of components, structures, and functions. This strategy not only augments the therapeutic efficacy and prognosis but also provides a valuable reference for the development and design of novel PNBMs. Researchers have also been engaged in the development of new nanomaterials with the objective of creating innovative biomaterials. Components, structure, function, and process constitute the fundamental paradigms in materials research and epitomize the intrinsic properties of materials.[25] By artfully combining diverse components, adjusting sizes, modifying structures, and transforming surface hydrophilicity, temporal control of PNBMs can be realized in response to the fluctuations in endogenous heterogeneous environments, thereby enabling the desired design functions during tumor nanotherapy. Additionally, through exogenous cascade response control, logic gate programming, and multifactorial response control, the PNBMs introduced into the body can be precisely manipulated in a time-sequenced manner to achieve targeted therapy.

Although PNBMs hold great promise for novel tumor nanotherapy, they are also confronted with several challenges. Tumors display substantial heterogeneity among patients, and the tumor microenvironment represents a complex system. PNBMs achieve temporal programmability by capitalizing on the gradient characteristics of the tumor microenvironment. It is of utmost importance to accurately synchronize with the tumor microenvironment to execute appropriate functions.[117–119] Secondly, the off-target effects of PNBMs frequently lead to serious side effects and undermine the treatment efficacy. In addition to striving for precise timing control in the performance of PNBMs, the biocompatibility and safety of the materials themselves are indispensable for their practical application.[120] Furthermore, the programmable design of PNBMs typically entails the transformation of structures and components. Therefore, it is crucial to comprehensively consider the compatibility and consistency between the material's biodegradation process and the programmable functioning process during the initial design phase.[121–123] This approach will expedite rapid degradation after treatment completion, thereby maximizing both functionality and safety.

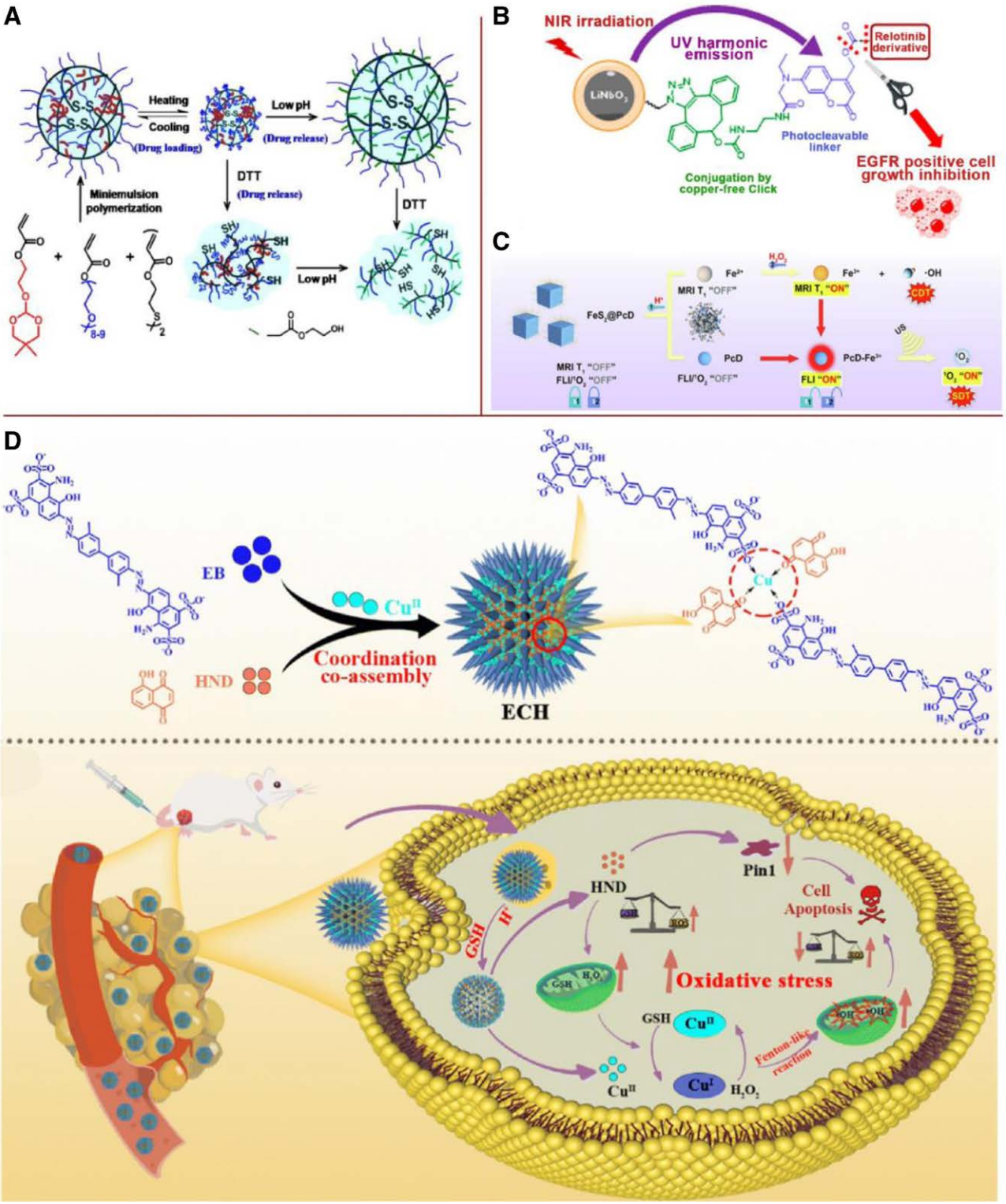

Figure 8. Multifactor response programmable PNBMs. (A) The construction of both thermoresponsive, reduction-sensitive, and pH-sensitive nanogels for an antitumor drug delivery system. Adapted with permission from Qiao et al.,[112] © 2011 Elsevier B.V. (B) Different wavelengths of laser light, including those in the near-infrared spectral range, are utilized as exogenous stimulants to modulate the morphology of the system. Adapted with permission from Fuller et al.,[113] © 2019 American Chemical Society. (C) The FeS_2@PcD nanoparticles are specifically designed to modulate the pH levels and concentrations of H_2O_2 within the tumor microenvironment, demonstrating a remarkable degree of targeted activation. Adapted with permission from Li et al.,[114] © 2023 Elsevier B.V. (D) Researchers have developed a spike-like programmable nanogenerator through a coordinated and driven coassembly process of EB, copper ions, and HND. It was able to promote rapid drug breakdown and controlled release under the dual stimulation of the acidic environment of lysosomes and endogenous GSH. Adapted with permission from Huang et al.,[115] © 2023 American Chemical Society.

Finally, PNBMs are still in a phase of rapid development, and comprehensively advancing their preclinical and clinical applications remains a paramount priority for the future.

With the continuous progress in nanotechnology, materiomics, artificial intelligence, and precision medicine, future PNBMs will become increasingly integrated, intelligent, sensitive, and personalized. In the foreseeable future, nanotechnology will permit precise control over the synthesis of PNBMs at the atomic level, facilitating the integration of intrinsic and extrinsic properties. This will give rise to more complex designs in terms of components, size, and functionality. Concurrently, the material genome will furnish foundational theoretical backing for the modular design of PNBMs. Complemented by the autonomy of artificial intelligence and predictive capabilities, the development of PNBMs will become more responsive and customized, potentially incorporating patient-specific tumor information for targeted design. We foresee that through persistent research and innovation, safer and more effective PNBMs will offer improved treatment options for cancer patients. These investigations will not only propel the field of cancer treatment forward but may also offer new insights and solutions for tackling other diseases.

Acknowledgments

The authors thank for the funding support by the union project of BUCT-CJFH biomedical center (PT2407, No. 2024-NHLHCRF-YXHZ-MS-05), the Fundamental Research Funds for the Central Universities (No. buctrc202419), the Postdoctoral Fellowship Program of CPSF (No. GZC20230196), the project of Science and Technology of Yinchuan (No. 2024SFZD004), and the National Natural Science Foundation of China (No. 22275013).

Conflicts of interests

The authors declare that they have no conflicts of interest.

References

[1] Gawne PJ, Ferreira M, Papaluca M, et al. New opportunities and old challenges in the clinical translation of nanotheranostics. *Nat Rev Mater*. 2023;8:783–798.
[2] Xie W, Guo Z, Zhao L, et al. The copper age in cancer treatment: from copper metabolism to cuproptosis. *Prog Mater Sci*. 2023;138:101145.
[3] Wang L, Zeng X, Yan G, et al. Biomimetic scaffolds with programmable pore structures for minimum invasive bone repair. *Nanoscale*. 2021;13(39):16680–16689.
[4] Senapati S, Mahanta AK, Kumar S, et al. Controlled drug delivery vehicles for cancer treatment and their performance. *Signal Transduct Target Ther*. 2018;3(1):7.
[5] Zhou Q, Liu Q, Wang Y, et al. Bridging smart nanosystems with clinically relevant models and advanced imaging for precision drug delivery. *Adv Sci*. 2024;11(14):e2308659.
[6] Luo M, Lee LKC, Peng B, et al. Delivering the promise of gene therapy with nanomedicines in treating central nervous system diseases. *Adv Sci*. 2022;9(26):e2201740.
[7] Sharma T, Gorivale S, Bhandari P. Targeted drug delivery in cancer using nanomaterials: advances and challenges. *J Nanoparticle Res*. 2024;26(6):127.
[8] Paroha S, Jain V, Rani L, et al. Nanoparticles for targeted drug delivery systems with cancer therapy in perspective. In: Rajput VS, Runthala A, eds. *Drugs and a Methodological Compendium: From Bench to Bedside*. Singapore: Springer Nature; 2023:313–334.
[9] Haleem A, Javaid M, Singh RP, et al. Applications of nanotechnology in medical field: a brief review. *Glob Health J*. 2023;7(2):70–77.
[10] Yoon H. Polymer nanomaterials in biomedicine. *Int J Mol Sci*. 2023;24(8):7480.
[11] Sorrentino C, Ciummo SL, Fieni C, et al. Nanomedicine for cancer patient-centered care. *MedComm*. 2024;5(11):e767.
[12] Duan X-P, Qin B-D, Jiao X-D, et al. New clinical trial design in precision medicine: discovery, development and direction. *Signal Transduct Target Ther*. 2024;9(1):1–29.
[13] Adams SA, Petersen C. Precision medicine: opportunities, possibilities, and challenges for patients and providers. *J Am Med Inform Assoc*. 2016;23(4):787–790.
[14] Wang J, Li Y, Nie G. Multifunctional biomolecule nanostructures for cancer therapy. *Nat Rev Mater*. 2021;6(9):766–783.
[15] Rawat N, Ahmad N, Raturi P, et al. Nanobiomaterials: exploring mechanistic roles in combating microbial infections and cancer. *Discov Nano*. 2023;18(1):158.
[16] Fathi-Achachelouei M, Knopf-Marques H, Ribeiro da Silva CE, et al. Use of nanoparticles in tissue engineering and regenerative medicine. *Front Bioeng Biotechnol*. 2019;7:113.
[17] Prabhu S, Poulose EK. Silver nanoparticles: mechanism of antimicrobial action, synthesis, medical applications, and toxicity effects. *Int Nano Lett*. 2012;2(1):32.
[18] Chen S-M, Wu K, Gao H-L, et al. Biomimetic discontinuous bouligand structural design enables high-performance nanocomposites. *Matter*. 2022;5(5):1563–1577.
[19] Liu S, Murata S, Kawamata I. DNA ring motif with flexible joints. *Micromachines*. 2020;11(11):987.
[20] Gu H, Chao J, Xiao S-J, et al. A proximity-based programmable DNA nanoscale assembly line. *Nature*. 2010;465(7295):202–205.
[21] Xie W, Zhang G, Guo Z, et al. Shape-controllable and kinetically miscible copper–palladium bimetallic nanozymes with enhanced fenton-like performance for biocatalysis. *Mater Today Bio*. 2022;16:100411.
[22] Speed SK, Gupta K, Peng Y-H, et al. Programmable polymer materials empowered by DNA nanotechnology. *J Polymer Sci*. 2023;61(16):1713–1729.
[23] Hu Y, Fan C. Nanocomposite DNA hydrogels emerging as programmable and bioinstructive materials systems. *Chem*. 2022;8(6):1554–1566.
[24] Xing Y, Dorey A, Jayasinghe L, et al. Highly shape- and size-tunable membrane nanopores made with DNA. *Nat Nanotechnol*. 2022;17(7):708–713.
[25] Xie W, Guo Z, Gao F, et al. Shape-, size- and structure-controlled synthesis and biocompatibility of iron oxide nanoparticles for magnetic theranostics. *Theranostics*. 2018;8(12):3284–3307.
[26] Sun X, Hua W, Liu X, et al. Programming of supercrystals using replicable DNA-functionalized colloids. *Angew Chem Int Ed Engl*. 2024;63(22):e202403492.
[27] Guo Z, Xie W, Zhang Q, et al. Photoactivation-triggered in situ self-supplied H_2O_2 for boosting chemodynamic therapy via layered double hydroxide-mediated catalytic cascade reaction. *Chem Eng J*. 2022;446:137310.
[28] Xie W, Gao Q, Guo Z, et al. Injectable and self-healing thermosensitive magnetic hydrogel for asynchronous control release of doxorubicin and docetaxel to treat triple-negative breast cancer. *ACS Appl Mater Interfaces*. 2017;9(39):33660–33673.
[29] Tang R, Fu Y-H, Gong B, et al. A chimeric conjugate of antibody and programmable DNA nanoassembly smartly activates T cells for precise cancer cell targeting. *Angew Chem Int Ed Engl*. 2022;61(36):e202205902.
[30] Li Y, Chen W, Koo S, et al. Innate immunity-modulating nanobiomaterials for controlling inflammation resolution. *Matter*. 2024;7(11):3811–3844.
[31] Chen F, Wang Y, Gao J, et al. Nanobiomaterial-based vaccination immunotherapy of cancer. *Biomaterials*. 2021;270:120709.
[32] Kubischok N. Assessing the future: past and present visions of nanomedicine. *Nanomedicine*. 2015;10(21):3195–3197.
[33] Yasir M, Mishra R, Tripathi AS, et al. Theranostics: a multifaceted approach utilizing nano-biomaterials. *Discover Nano*. 2024;19(1):35.
[34] Gilbert C, Tang T-C, Ott W, et al. Living materials with programmable functionalities grown from engineered microbial co-cultures. *Nat Mater*. 2021;20(5):691–700.
[35] Tang F, Li L, Chen D. Mesoporous silica nanoparticles: synthesis, biocompatibility and drug delivery. *Adv Mater*. 2012;24(12):1504–1534.
[36] Chaudhary Z, Subramaniam S, Khan GM, et al. Encapsulation and controlled release of resveratrol within functionalized mesoporous silica nanoparticles for prostate cancer therapy. *Front Bioeng Biotechnol*. 2019;7:225.
[37] Mamidi N, Mostafavi E, Yallapu MM. Editorial: exploring the potential of nanobiomaterials in biomedical engineering: assessing biocompatibility, toxicity, and future prospects. *Front Chem*. 2024;12:1461483.

[38] Cucchi D, Menon A, Aliprandi A, et al. Patient-specific instrumentation affects rotational alignment of the femoral component in total knee arthroplasty: a prospective randomized controlled trial. *Orthop Surg*. 2019;11(1):75–81.
[39] Lim B, Yin Y, Ye H, et al. Reprogramming synthetic cells for targeted cancer therapy. *ACS Synth Biol*. 2022;11(3):1349–1360.
[40] Stejskalova A, Kiani MT, Almquist BD. Programmable biomaterials for dynamic and responsive drug delivery. *Exp Biol Med (Maywood)*. 2016;241(10):1127–1137.
[41] Yang Y, Liu Q, Wang M, et al. Genetically programmable cell membrane-camouflaged nanoparticles for targeted combination therapy of colorectal cancer. *Signal Transduct Target Ther*. 2024;9(1):1–16.
[42] Allen TM, Cullis PR. Liposomal drug delivery systems: from concept to clinical applications. *Adv Drug Deliv Rev*. 2013;65(1):36–48.
[43] Li S, Xing R, van Hest JCM, et al. Peptide-based supramolecular assembly drugs toward cancer theranostics. *Expert Opin Drug Deliv*. 2022;19(7):847–860.
[44] Chang R, Zhao L, Xing R, et al. Functional chromopeptide nanoarchitectonics: molecular design, self-assembly and biological applications. *Chem Soc Rev*. 2023;52(8):2688–2712.
[45] Yan Y, Ding H. pH-responsive nanoparticles for cancer immunotherapy: a brief review. *Nanomaterials*. 2020;10(8):1613.
[46] Xue L, Thatte AS, Mai D, et al. Responsive biomaterials: optimizing control of cancer immunotherapy. *Nat Rev Mater*. 2024;9(2):100–118.
[47] Xie W, Ye J, Guo Z, et al. Ultrafast fabrication of iron/manganese co-doped bismuth trimetallic nanoparticles: a thermally aided chemodynamic/radio-nanoplatform for low-dose radioresistance. *ACS Appl Mater Interfaces*. 2022;14(19):21931–21944.
[48] Zhang D-Y, Cao R-G, Cheng Y-J, et al. Programming lipopeptide nanotherapeutics for tandem treatment of postsurgical infection and melanoma recurrence. *J Control Release*. 2023;362:565–576.
[49] Su L, Jin D, Wang Y, et al. Modularized microrobot with lock-and-detachable modules for targeted cell delivery in bile duct. *Sci Adv*. 2023;9(50):eadj0883.
[50] Abdelmawla A, Guo S, Zhang L, et al. Pharmacological characterization of chemically synthesized monomeric Phi29 pRNA nanoparticles for systemic delivery. *Mol Ther*. 2011;19(7):1312–1322.
[51] Krishnan N, Jiang Y, Zhou J, et al. A modular approach to enhancing cell membrane-coated nanoparticle functionality using genetic engineering. *Nat Nanotechnol*. 2024;19(3):345–353.
[52] Mout R, Bretherton RC, Decarreau J, et al. De novo design of modular protein hydrogels with programmable intra- and extracellular viscoelasticity. *Proc Natl Acad Sci USA*. 2024;121(6):e2309457121.
[53] Ma X, Liang X, Li Y, et al. Modular-designed engineered bacteria for precision tumor immunotherapy via spatiotemporal manipulation by magnetic field. *Nat Commun*. 2023;14(1):1606.
[54] Sun L, Liu H, Ye Y, et al. Smart nanoparticles for cancer therapy. *Signal Transduct Target Ther*. 2023;8(1):1–28.
[55] Chang R, Zou Q, Zhao L, et al. Amino-acid-encoded supramolecular photothermal nanomedicine for enhanced cancer therapy. *Adv Mater*. 2022;34(16):2200139.
[56] Wang C, Xu J, Cheng X, et al. Anti-lymphangiogenesis for boosting drug accumulation in tumors. *Signal Transduct Target Ther*. 2024;9(1):1–15.
[57] Lu Y, Zhang E, Yang J, et al. Strategies to improve micelle stability for drug delivery. *Nano Res*. 2018;11(10):4985–4998.
[58] Rybczynski N, Gosse JC, Richard Harington C, et al. Mid-pliocene warm-period deposits in the high arctic yield insight into camel evolution. *Nat Commun*. 2013;4(1):1550.
[59] Ma H, Mu X, Tang Y, et al. Programmable multistage small-molecule nano-photosensitizer for multimodal imaging-guided photothermal therapy. *Acta Biomater*. 2023;157:408–416.
[60] Lajoie P, Guay G, Dennis JW, et al. The lipid composition of autophagic vacuoles regulates expression of multilamellar bodies. *J Cell Sci*. 2005;118(9):1991–2003.
[61] Cheng F, Huang Q-F, Li Y-H, et al. Combined chemo and photo therapy of programmable prodrug carriers to overcome delivery barriers against nasopharyngeal carcinoma. *Biomater Adv*. 2023;151:213451.
[62] Yang Z, Fu X, Zhou L, et al. Chem-inspired synthesis of injectable metal–organic hydrogels for programmable drug carriers, hemostasis and synergistic cancer treatment. *Chem Eng J*. 2021;423:130202.
[63] Wang L, Li S-Y, Jiang W, et al. Polyphosphoestered nanomedicines with tunable surface hydrophilicity for cancer drug delivery. *ACS Appl Mater Interfaces*. 2020;12(29):32312–32320.
[64] Lee J, Davaa E, Jiang Y, et al. Pheophorbide A and SN38 conjugated hyaluronan nanoparticles for photodynamic- and cascadic chemotherapy of cancer stem-like ovarian cancer. *Carbohydr Polym*. 2022;289:119455.
[65] Borkowska M, Siek M, Kolygina DV, et al. Targeted crystallization of mixed-charge nanoparticles in lysosomes induces selective death of cancer cells. *Nat Nanotechnol*. 2020;15(4):331–341.
[66] Huang W, Zhao H, Wan J, et al. pH- and photothermal-driven multistage delivery nanoplatform for overcoming cancer drug resistance. *Theranostics*. 2019;9(13):3825–3839.
[67] Hu C, Yang X, Liu R, et al. Coadministration of iRGD with multistage responsive nanoparticles enhanced tumor targeting and penetration abilities for breast cancer therapy. *ACS Appl Mater Interfaces*. 2018;10(26):22571–22579.
[68] Mu X, Wu F, Tang Y, et al. Boost photothermal theranostics via self-assembly-induced crystallization (SAIC). *Aggregate*. 2022;3(5):e170.
[69] Padmajan Sasikala S, Lim J, Kim IH, et al. Graphene oxide liquid crystals: a frontier 2D soft material for graphene-based functional materials. *Chem Soc Rev*. 2018;47(16):6013–6045.
[70] Luo Y, Li Z, Zhu C, et al. Graphene-like metal-free 2D nanosheets for cancer imaging and theranostics. *Trends Biotechnol*. 2018;36(11):1145–1156.
[71] Chen W, Ouyang J, Liu H, et al. Black phosphorus nanosheet-based drug delivery system for synergistic photodynamic/photothermal/chemotherapy of cancer. *Adv Mater*. 2017;29(5):1603864.
[72] Pillai PP, Kowalczyk B, Kandere-Grzybowska K, et al. Engineering Gram selectivity of mixed-charge gold nanoparticles by tuning the balance of surface charges. *Angew Chem Int Ed*. 2016;55(30):8610–8614.
[73] Pillai PP, Huda S, Kowalczyk B, et al. Controlled pH stability and adjustable cellular uptake of mixed-charge nanoparticles. *J Am Chem Soc*. 2013;135(17):6392–6395.
[74] Rao A, Roy S, Unnikrishnan M, et al. Regulation of interparticle forces reveals controlled aggregation in charged nanoparticles. *Chem Mater*. 2016;28(7):2348–2355.
[75] Al-Lazikani B, Banerji U, Workman P. Combinatorial drug therapy for cancer in the post-genomic era. *Nat Biotechnol*. 2012;30(7):679–692.
[76] Zhao H, Lv J, Li F, et al. Enzymatical biomineralization of DNA nanoflowers mediated by manganese ions for tumor site activated magnetic resonance imaging. *Biomaterials*. 2021;268:120591.
[77] Gregory JV, Vogus DR, Barajas A, et al. Programmable delivery of synergistic cancer drug combinations using bicompartmental nanoparticles. *Adv Healthc Mater*. 2020;9(21):2000564.
[78] Chen X, Zhang X, Zhang L, et al. Amphiphilic janus nanoparticles for imaging-guided synergistic chemo-photothermal hepatocellular carcinoma therapy in the second near-infrared window. *Nanoscale*. 2021;13(7):3974–3982.
[79] Li G, Xia F, Xiao H, et al. Fine-tuning the structure-tolerance-antitumor efficacy axis of prodrug nanoassemblies via branched aliphatic functionalization. *Nano Res*. 2023;17:2908–2918.
[80] Li Y, Wang L, Liang J, et al. Hierarchical heterostructure of ZnO@TiO2 hollow spheres for highly efficient photocatalytic hydrogen evolution. *Nanoscale Res Lett*. 2017;12(1):531.
[81] Di Martino A, Ozaltin K, Trusova ME, et al. Multidrug delivery system based on polysaccharide nanocomplexes for controlled delivery of a combination of chemotherapeutics. *J Drug Delivery Sci Technol*. 2019;50:90–98.
[82] Zhou Y-Y, Xu Y-C, Yao Z-F, et al. Visualizing the multi-level assembly structures of conjugated molecular systems with chain-length dependent behavior. *Nat Commun*. 2023;14(1):3340.
[83] Choudhury S, Bajaj M, Dash T, et al. Multilevel inverter: a survey on classical and advanced topologies, control schemes, applications to power system and future prospects. *Energies*. 2021;14(18):5773.
[84] Zhao Q, Dunlop JWC, Qiu X, et al. An instant multi-responsive porous polymer actuator driven by solvent molecule sorption. *Nat Commun*. 2014;5(1):4293.
[85] Pascucci L, Coccè V, Bonomi A, et al. Paclitaxel is incorporated by mesenchymal stromal cells and released in exosomes that inhibit in vitro tumor growth: a new approach for drug delivery. *J Control Release*. 2014;192:262–270.
[86] Yao S, Li X, Liu J, et al. Maximized nanodrug-loaded mesenchymal stem cells by a dual drug-loaded mode for the systemic treatment of metastatic lung cancer. *Drug Deliv*. 2017;24(1):1372–1383.
[87] Dai T, Yang E, Sun Y, et al. Preparation and drug release mechanism of CTS-TAX-NP-MSCs drug delivery system. *Int J Pharm*. 2013;456(1):186–194.
[88] Sadhukha T, O'Brien TD, Prabha S. Nano-engineered mesenchymal stem cells as targeted therapeutic carriers. *J Control Release*. 2014;196:243–251.
[89] Yang G, Xu L, Chao Y, et al. Hollow MnO_2 as a tumor-microenvironment-responsive biodegradable nano-platform for combination therapy favoring antitumor immune responses. *Nat Commun*. 2017;8(1):902.

[90] Li Y, Gong S, Pan W, et al. A tumor acidity activatable and Ca2+-assisted immuno-nanoagent enhances breast cancer therapy and suppresses cancer recurrence. *Chem Sci*. 2020;11(28):7429–7437.
[91] Zhang H, Chen W, Gong K, et al. Nanoscale zeolitic imidazolate framework-8 as efficient vehicles for enhanced delivery of CpG oligodeoxynucleotides. *ACS Appl Mater Interfaces*. 2017;9(37):31519–31525.
[92] Vallejo-Sánchez D, Amo-Ochoa P, Beobide G, et al. Chemically resistant, shapeable, and conducting metal-organic gels and aerogels built from dithiooxamidato ligand. *Adv Funct Mater*. 2017;27(15):1605448.
[93] Kim J, Lee D. Crisscrossing coordination networks: ligand doping to control the chemomechanical properties of stimuli-responsive metallogels. *Chem Sci*. 2019;10(13):3864–3872.
[94] Huo S-H, Yan X-P. Metal–organic framework MIL-100(Fe) for the adsorption of malachite green from aqueous solution. *J Mater Chem*. 2012;22(15):7449.
[95] Su Y-C, Burnouf P-A, Chuang K-H, et al. Conditional internalization of PEGylated nanomedicines by PEG engagers for triple negative breast cancer therapy. *Nat Commun*. 2017;8(1):15507.
[96] Shi J, Kantoff PW, Wooster R, et al. Cancer nanomedicine: progress, challenges and opportunities. Nat Rev Cancer. 2017;17(1):20–37.
[97] Sun W, Hu Q, Ji W, et al. Leveraging physiology for precision drug delivery. *Physiol* Rev. 2017;97:189–225.
[98] Cedervall T, Lynch I, Lindman S, et al. Understanding the nanoparticle–protein corona using methods to quantify exchange rates and affinities of proteins for nanoparticles. *Proc Natl Acad Sci USA*. 2007;104(7):2050–2055.
[99] Ritz S, Schöttler S, Kotman N, et al. Protein corona of nanoparticles: distinct proteins regulate the cellular uptake. *Biomacromolecules*. 2015;16(4):1311–1321.
[100] Xie W, Lu J, Guo Z, et al. Necroptosis-elicited host immunity: GOx-loaded MoS2 nanocatalysts for self-amplified chemodynamic immunotherapy. *Nano Res*. 2022;15(3):2244–2253.
[101] Abed A, Derakhshan M, Karimi M, et al. Platinum nanoparticles in biomedicine: preparation, anti-cancer activity, and drug delivery vehicles. *Front Pharmacol*. 2022;13:797804.
[102] Hassan AHA, Abdi I, Alsherif EA, et al. Species-specific ecotoxicity of platinum nanoparticles to two cyanobacteria. *Mar Pollut Bull*. 2024;209:117054.
[103] Shi H, Xu M, Zhu J, et al. Programmed co-delivery of platinum nanodrugs and gemcitabine by a clustered nanocarrier for precision chemotherapy for NSCLC tumors. *J Mater Chem B*. 2020;8(2):332–342.
[104] Li Z, Shi H, Xie H, et al. Tri-component programmable nanoregulator with three-pronged penetration boosts immunotherapy of triple-negative breast cancer. *Chem Eng J*. 2022;439:135712.
[105] Tang L, Yang Z, Zhou Z, et al. A logic-gated modular nanovesicle enables programmable drug release for on-demand chemotherapy. Theranostics. 2019;9(5):1358–1368.
[106] Zhou H, He G, Sun Y, et al. Cryptobiosis-inspired assembly of "AND" logic gate platform for potential tumor-specific drug delivery. *Acta Pharm Sin B*. 2021;11:534–543.
[107] Li C, Wu Y, Zhu Y, et al. Molecular motor-driven light-controlled logic-gated K+ channel for cancer cell apoptosis. *Adv Mater*. 2024;36(19):2312352.
[108] Bai L, Wang X, Song F, et al. "AND" logic gate regulated pH and reduction dual-responsive prodrug nanoparticles for efficient intracellular anticancer drug delivery. *Chem Commun*. 2015;51(1):93–96.
[109] Xie W, Guo Z, Gao Q, et al. Manganese-doped layered double hydroxide: a biodegradable theranostic nanoplatform with tumor microenvironment response for magnetic resonance imaging-guided photothermal therapy. *ACS Appl Bio Mater*. 2020;3(9):5845–5855.
[110] Xie W, Guo Z, Cao Z, et al. Manganese-based magnetic layered double hydroxide nanoparticle: a pH-sensitive and concurrently enhanced T1/T2-weighted dual-mode magnetic resonance imaging contrast agent. *ACS Biomater Sci Eng*. 2019;5(5):2555–2562.
[111] Xie W, Gao Q, Wang D, et al. Melatonin potentiates inside-out nano-thermotherapy in human breast cancer cells: a potential cancer target multimodality treatment based on melatonin-loaded nanocomposite particles. *Int J Nanomedicine*. 2017;12:7351–7363.
[112] Qiao Z-Y, Zhang R, Du F-S, et al. Multi-responsive nanogels containing motifs of ortho ester, oligo(ethylene glycol) and disulfide linkage as carriers of hydrophobic anti-cancer drugs. *J Control Release*. 2011;152(1):57–66.
[113] Fuller EG, Sun H, Dhavalikar RD, et al. Externally triggered heat and drug release from magnetically controlled nanocarriers. *ACS Appl Polym Mater.* 2019;1(2):211–220.
[114] Li D, Pan J, Xu S, et al. Programmable phthalocyanine-iron-based nanoreactor for fluorescence/magnetic resonance dual-modality imaging-guided sono/chemodynamic therapies. *Chem Eng* J. 2023;452:139330.
[115] Huang L, Wu F, Wang Q, et al. TME-triggered copper-coordinated engineered programmable nanogenerators for on-demand cascade-amplifying oxidative stress. *J Mater Chem B*. 2023;11(16):3679–3692.
[116] Gheata A, Gaulier G, Campargue G, et al. Photoresponsive nanocarriers based on lithium niobate nanoparticles for harmonic imaging and on-demand release of anticancer chemotherapeutics. *ACS Nanosci Au*. 2022;2(4):355–366.
[117] de Lázaro I, Mooney DJ. Obstacles and opportunities in a forward vision for cancer nanomedicine. *Nat Mater*. 2021;20(11):1469–1479.
[118] Fan D, Cao Y, Cao M, et al. Nanomedicine in cancer therapy. *Signal Transduct Target Ther*. 2023;8(1):1–34.
[119] Li X, Montague EC, Pollinzi A, et al. Design of smart size-, surface-, and shape-switching nanoparticles to improve therapeutic efficacy. *Small*. 2022;18(6):2104632.
[120] Zhang F, Zhang Z, Yang W, et al. Engineering autologous cell-derived exosomes to boost melanoma-targeted radio-immunotherapy by cascade cGAS-STING pathway activation. *Small*. 2024;n/a(n/a):2408769.
[121] Xie W, Ye J, Guo Z, et al. TME-responded full-biodegradable nanocatalyst for mitochondrial calcium overload-induced hydroxyl radical bursting cancer treatment. *Chem Eng J*. 2022;438:135372.
[122] Guo Z, Gao X, Lu J, et al. Apoptosis and paraptosis induced by disulfiram-loaded Ca2+/Cu2+ dual-ions nano trap for breast cancer treatment. *ACS Nano*. 2024;18(9):6975–6989.
[123] Huang H, Xie W, Wan Q, et al. A self-degradable conjugated polymer for photodynamic therapy with reliable postoperative safety. *Adv Sci*. 2022;9(4):e2104101.

How to cite this article: Wang J, Hou J, Lu H, Bai S, Chen Y, Yang W, Wang S, Li G, Wei Y, Wang X, Xie W. Engineering programmable nanobiomaterials (PNBMs) for cancer nanotherapy. MedMat 2025;2(1):e00011. doi: 10.1097/mm9.0000000000000011